Ecosystem metabolism in the lower Columbia and Willamette Rivers, USA: Insights into the juvenile salmonid food web

Tawnya D. Peterson[1,2]*, Nikolai M. Danilchik[2], and Joseph A. Needoba[1,2]

[1]Oregon Health & Science University-Portland State University School of Public Health, VPT, 1810 SW 5th Ave., Portland, Oregon 97201

[2]Institute of Environmental Health, Oregon Health & Science University, 3181 SW Sam Jackson Park Rd., Portland, Oregon 97239

*Corresponding Author
E-mail: petertaw@ohsu.edu

Abstract

The Columbia River and its major tributary, the Willamette River, are large systems impacted by human activities, including the installation of hydroelectric dams. Hourly measurements of dissolved oxygen (DO) from *in situ* sensors and laboratory incubations showed that daily net ecosystem production (NEP) was slightly positive in the Columbia, with annual NEP of 121.30 gC m^{-2} y^{-1}. In the Willamette, we observed high gross primary production (GPP) and positive daily NEP during the summer months but slightly negative daily NEP during winter and spring, with annual NEP equal to -16.67 gC m^{-2} y^{-1}. Our estimates of annual NEP in both the Columbia and the Willamette far exceeded the global average reported for temperate rivers of -260 gC m^{-2} y^{-1}. Generalized additive regression modeling showed that variation GPP and ecosystem respiration (ER) could be explained by river discharge, chlorophyll concentration, temperature, and nitrate concentration in the Columbia River (83.0% and 73.8% of deviance in GPP and ER explained, respectively). In the Willamette, variation in GPP was associated with chlorophyll and temperature (41.6% of deviance explained), while ER variation tracked temperature alone (31.6% of deviance explained). The light attenuation coefficient (K_d) determined from vertical irradiance profiles was influenced by turbidity in both rivers, with chlorophyll accounting for 7.7% of the variation in turbidity in the Willamette and 43.5% in the Columbia. A comparison of GPP rates determined from *in situ* and bottle data suggest that the relative contribution of phytoplankton versus vascular plants to GPP is modulated by hydrologic variation. The data lend support for classifying the Columbia as a 'green' river, where annual areal primary production exceeds respiration and food webs are supported by autochthonous production. The Willamette displayed characteristics of both a green and a brown river, depending on the

42 season, with a shift from negative to positive NEP values from winter to summer and net
43 negative values at an annual scale.

Introduction

Characterization and quantification of aquatic primary production and respiration constitute fundamental aspects of ecosystem science that are crucial for understanding and modeling the global carbon cycle (1-4), for predicting coastal hypoxia risk (5, 6), and for tracking water quality and energy flow in aquatic habitats (7-9). Until recently (10, 11), comparatively few investigations of water column primary productivity and ecosystem metabolism have been conducted in rivers relative to other aquatic systems, resulting in gaps in knowledge about their influence on global carbon budgets and response to climate change (12). This is particularly true for large rivers, for which much less is known than streams or small rivers (13). In part, this reflects the challenge of making observations in highly dynamic large-river ecosystems (14) or reproducing complex environmental conditions in the laboratory (15). With the availability of robust *in situ* sensors capable of collecting continuous, high-resolution data (16-19), it is increasingly possible to observe temporal variations in ecosystem constituents that provide better insight into the drivers and characteristics of riverine primary production (20, 21).

An important application of *in situ* sensors for improved understanding of aquatic carbon cycling is the determination of net ecosystem metabolism, or NEM (22), also conceptualized as net ecosystem production (NEP). NEM, or NEP, is the balance between gross primary production (GPP) and ecosystem respiration (ER) in a 24 h period as determined by changes in dissolved oxygen (DO), usually from hourly data (23-25). NEP is useful for characterizing the trophic state of an ecosystem: positive values indicate that production of organic matter (OM) exceeds respiration, which influences food webs, energy flow, and water quality. When GPP < ER (i.e., negative NEP), the system is a net sink for O_2

and biological production is fueled by allochthonous organic matter rather than autochthonously produced organic matter (22, 26). The trophic status of rivers provides an indicator of a system's susceptibility to eutrophication (27, 28) and informs global carbon budget assessments (29), which supports resource management and climate mitigation strategies. New analytic tools to aid calculation of ecosystem metabolism have advanced our understanding of controls on biological production in river systems (30, 31); however, large rivers are not always well characterized by the tools that aid in determining ecosystem productivity for streams and smaller rivers (13), underscoring challenges in deriving estimates of gross primary productivity (GPP), ecosystem respiration (ER), or net ecosystem production (NEP) in these systems.

The Columbia River is a large and complex system with competing social-ecological-economic interests, including recreation, culture, critical habitat, agriculture, and shipping (32). The dramatic decline of ecologically and culturally important west coast salmonid populations over the past several decades has motivated substantial efforts to restore critical habitats that support ESA-listed stocks during their juvenile stages (33, 34). River restoration efforts have increasingly acknowledged the importance of habitat features, food webs, and ecological processes (35-38) and their sensitivity to climate change (39, 40). The complex lifecycles of anadromous fish, including salmonids, require that restoration efforts take an ecosystem approach that includes habitat characterization (41, 42); determination of NEP supports these efforts by yielding insight into organic matter sources and availability for pelagic food webs, as well as through identification of potential drivers of poor water quality that negatively impact fish growth and survival.

The Columbia River has been heavily modified by the installation of hydroelectric dams along its mainstem between 1933 and 1984 (43). Aside from presenting barriers to fish passage, hydroelectric dams influence carbon cycling and flow to the ocean through modification of flow regimes, water clarity, and residence times (44, 45) that accompany the sequence of dams and impoundments along the Columbia's mainstem, which have fundamentally altered the hydrograph and riverine ecosystems (46-49). One aspect of the decline of anadromous species that has received attention is an apparent shift from detritus-based to a phytoplankton-based food webs that is thought to have accompanied the installation of major hydroelectric dams (50-52). Silt trapping in impoundments behind major dams tends to lower turbidity and increase light penetration through the water column (7, 51, 53), opening a niche for phytoplankton and increasing autochthonous production of organic carbon. A shift in riverine organic matter from detritus-dominated to a mix of allochthonous and autochthonous sources has been implicated in changes in biogeochemical cycles (54) – similar to effects more generally observed in other dammed systems (44, 45, 55, 56) – as well as food web characteristics (52), fish assemblages (57, 58) and ultimately a decline in salmonid stocks (59-61) in the lower river and estuary. Although phytoplankton are considered an important source of energy to consumers in large rivers generally (62, 63), the significance of a shift toward greater phytoplankton production as well as other indirect impacts of dams on salmon survival in the Columbia remain poorly understood (64, 65).

One of the goals of the present study of ecosystem metabolism was to characterize the rhythms of metabolism in the Columbia and Willamette Rivers and determine the balance of autotrophy versus heterotrophy in these systems to better understand implications of a shift from detritus-based to phytoplankton-based food webs in the Columbia River. In contrast to

the Columbia, the Willamette River has fewer major dams and other barriers to flow than the Columbia and is characterized by high turbidity and high nutrient concentrations from agricultural inputs along the productive Willamette Valley (31, 66, 67), providing additional insights into environmental controls on ecosystem metabolism.

In this study, we used *in situ* dissolved oxygen (DO) sensors to determine daily and annual rates of gross primary production (GPP), ecosystem respiration (ER), and NEP between July 2017 and July 2018 in two large rivers, the Columbia and its major tributary, the Willamette, to characterize their productivity regimes as a foundational element of salmonid habitat. This work informs broader efforts to characterize the salmon food web as part of the Lower Columbia Estuary Partnership (LCEP)'s Ecosystem Monitoring Program (EMP) (https://www.estuarypartnership.org/) and supports improved understanding of the carbon budget in these systems.

Materials and Methods

The Columbia River system. The Columbia River is the fourth largest in North America by flow, draining a land area of 668,000 km^2 that encompasses seven U.S. states and one Canadian province. The river has been extensively dammed for hydroelectricity generation and flood control with 18 major hydroelectric dams in the Columbia and lower Snake Rivers that have created a series impoundments connected by river flow; the Columbia includes more than 250 reservoirs along its length (https://www.nwd.usace.army.mil/crwm/cr-dams/).

The Willamette River, a major tributary of the Columbia, is the 19th largest in the United States by volume, draining 11,487 square miles (68) and accounting for 12-15% of

the Columbia River flow downstream of the confluence. Similar to the Columbia, flows in the Willamette and its tributaries are highly regulated, with 20 dams operated mainly for navigation and flood control.

Sensor locations and sample sites. We collected hourly data from *in situ* oxygen sensors and co-located water quality parameters (temperature, conductivity, turbidity, chlorophyll) at two sites: one in the Columbia River as part of the Lower Columbia Estuary Partnership's Ecosystem Monitoring Program and one in the Willamette River. The Columbia River sensor platform is part of a network of sensors operated by the Columbia River Inter-Tribal Fish Commission (CRITFC)'s Center for Coastal Margin Observation and Prediction (CMOP). The sensor network is referred to as the Science & Technology University Research Network (SATURN) (www.cmop.critfc.org) (69); the Columbia River site is referred to as SATURN-08 and is located at the Port of Camas-Washougal in the Columbia River (river mile 122, river km 196) upstream of the Columbia-Willamette confluence. The sensor package consisted of a metal frame with sensors attached; the frame was mounted on a floating dock that extends ~100-125 m into the river channel. The Willamette River site is known as SATURN-06 and is maintained by the U. S. Geological Survey (station ID 14211720); the sensor package is fixed to the Morrison Bridge in Portland, Oregon (river mile 12.8, river km 21; **Fig. 1**). SATURN-08 sensor data were downloaded from http://columbia.loboviz.com, and SATURN-06 data were acquired from the U.S. Geological Survey [https://waterdata.usgs.gov/nwis/inventory/?site_no=14211720]. All sensors were serviced by the manufacturer annually and calibrated prior to deployment according to manufacturer recommendations. Dissolved oxygen sensors underwent 2-point calibration in the laboratory before deployment. The sensors were cleaned every 3-4 weeks

during the deployment period and data were downloaded and subject to quality control checks.

Figure 1. Map of the Columbia River estuary from the Bonneville Dam to the river mouth, including study area. The locations of sensor platforms (SATURN-05, -06, -08) and water sampling (Willamette Park) are indicated in colored circles. The location of Bonneville Dam is included for reference. SATURN-05 is also known as Beaver Army Terminal; SATURN-06 is referred to as 'Camas, Washington' for its location at the Port of Camas; and SATURN-08 is in the Willamette River at Morrison Bridge in Portland, Oregon.

In addition to collecting sensor data, we determined rates of primary production and respiration through laboratory incubation experiments carried out in a temperature-controlled walk-in environmental chamber in the laboratory (described below). Weekly 1-L grab samples were collected in triplicate for the incubations and for measuring dissolved nutrients (nitrate, phosphate) at the sensor site at Camas and <4 km upstream of the SATURN-06 sensor package in the Willamette River at a site on the South Waterfront of Portland, Oregon (45°28'32"N, 122°40'04"W). Vertical profiles of temperature-conductivity-dissolved oxygen-depth were performed at sites in close proximity to the *in situ* sensors (co-located with the SATURN-08 sensor package in the Columbia and on the South Waterfront (SWF).

Light, conductivity, temperature, and dissolved oxygen profiles. A LiCor LI-1500 light sensor (LiCor Inc., Lincoln, NE) was attached to a SonTek CastAway CTD (conductivity, temperature, depth; Yellow Springs Instruments Inc., Yellow Springs, OH)

unit to collect weekly measurements of photosynthetically active radiation (PAR) through the water column at both the Columbia and Willamette sites. In addition, we collected vertical profile data through the water column at the Columbia site using a YSI (Yellow Springs Instruments Inc., Yellow Springs, OH) sonde equipped with an OBOD 626401 probe to measure dissolved oxygen concentration and saturation relative to the atmosphere during spring-summer in 2018 (15 weeks). Both the CTD unit plus light sensor and DO probe were lowered three times to the river bottom to measure light, conductivity, temperature, and DO through the water column following surface equilibration (~30 s). The profile data were binned to 1 m depth intervals in the Columbia River and 0.5 m intervals in the Willamette River (SWF). Data from the three casts were averaged to produce vertical profiles of all parameters for each day and site.

The light attenuation coefficient, K_d, was calculated from vertical profiles of PAR data according to:

$$K_d = \frac{-\ln\left(\frac{I_z}{I_0}\right)}{z}$$

where I_0 is the surface irradiance (μmol m^{-2} s^{-1}), I_z is the irradiance at depth z, and z is the depth (in m).

Gross primary production, ecosystem respiration, and net ecosystem production. Gross primary production (GPP), Ecosystem Respiration (ER), and Net Ecosystem Production (NEP) were determined from (1) continuous *in situ* sensor DO data and from (2) bottle incubation experiments.

Continuous data were used to determine GPP, ER, and NEP according to the single-station, open water method (23, 30, 70, 71), where daily GPP, ER, and NEP rates were

204 determined from hourly changes in biologically derived oxygen (BDO) (22, 25). We
205 subtracted abiotic oxygen flux, the product of atmosphere-surface water gas diffusion, which
206 is a function of water temperature, wind speed, and current velocity (72, 73). Wind speed
207 data used for determining k_{wind}, the gas transfer velocity associated with wind-driven friction,
208 at SATURN-08 were downloaded from the weather station at the Troutdale Airport (station
209 ID: GHCND:USW00024242; 45.55098°N, -122.40984°W, https://www.ncdc.noaa.gov/cdo-
210 web/datasets/GHCND/stations/GHCND:USW00024242/detail), and for SATURN-06 from
211 the Portland International Airport (GHCND:USW00024229; 45.59578°N, -122.60919°W;
212 https://www.ncdc.noaa.gov/cdo-
213 web/datasets/GHCND/stations/GHCND:USW00024229/detail), accessed from the Climate
214 Data Online interface provided by the Global Historical Climatology Network's daily
215 database, managed and maintained by NOAA's National Centers for Environmental
216 Information (NCEI). USGS water velocity data for the Willamette site were recorded at
217 SATURN-06 (site code 14211720; https://waterdata.usgs.gov/nwis/uv?14211720); velocity
218 measurements for the SATURN-08 site were obtained from the USGS at site 14144700 in
219 Vancouver, WA (https://waterdata.usgs.gov/nwis/uv?14144700). The gas transfer velocity
220 (k) was computed according to Wanninkhof (73) normalized to a Schmidt number (Sc) of
221 660 and included k_{wind} and k_{flow} components.

222 We estimated ER by calculating the average hourly change in DO during night hours
223 in the absence of photosynthesis and assuming this rate was constant over 24 h. Daily-
224 integrated ER was thus determined by multiplying the hourly nighttime rate by 24 h. Daily-
225 integrated GPP was estimated from addition of the sum of daytime hourly DO changes
226 during the day and the sum of hourly ER during the day (ER_{Day}):

$$GPP = \Sigma\Delta DO_{Day} + |\Sigma ER_{Day}| \quad (1)$$

where ER_{Day} is the product of average nighttime hourly respiration times the number of daylight hours and $\Sigma\Delta DO_{Day}$ is the sum of hourly DO changes observed during the day, or daily net primary production (NPP).

NEP is net ecosystem production, which refers to the daily balance of GPP and ER (NEP = GPP – ER). NPP refers to the amount of primary production minus losses to respiration; that is, on an hourly basis, NPP reflects net production of biologically fixed carbon); in contrast, NEP considers the balance of primary production and respiration for the system for a 24 h period. Therefore, daily NEP is calculated from:

$$NEP = GPP - |\Sigma ER_{24h}| \quad (2)$$

GPP is gross primary productivity that takes place during the day and is reported as a daily rate, ΣER_{24h} is the total amount of respiration that occurs in 24 h, and NEP is the balance between the two. Thus, NEP will always be lower than NPP.

For calculations of GPP, NEP, and ER, O_2 measurements were converted to units of carbon (C) using a photosynthetic quotient of 1.3; a respiratory quotient of 0.85 was used in ER calculations (74).

To consider the impact of inaccuracies in depth on NEP estimates, we compared calculations of respiration with and without the k_{flow} term, which parameterizes the influence of bottom friction on velocity distributions in the flow field, as well as various simulated

current velocities (**Fig. S1**). There were negligible differences in NEP with or without k_{flow} at the velocities encountered during the study period. We also assumed that the influences of ground water and chemical oxidation were negligible at the sites, given the large surface flow volumes in both the Columbia and Willamette Rivers, which should overwhelm inputs from groundwater.

Bonneville is a run-of-the-river dam, with spill discharge ranging from < 3 kcfs (84.95 m^3 s^{-1}) in the fall and winter months to >300 kcfs (8495 m^3 s^{-1}) in the spring during the freshet. Dam operations often lead to the injection of dissolved gases from the atmosphere into waters when the spillway is operational (13, 75). The same process occurs in association with natural features such as waterfalls and pressure-driven supersaturation could be included as another term in the determination of the gas transfer velocity, *k* (73). Roley et al., (2023) recommended applying a correction to account for excess oxygen in waters downstream of dam structures, so we consulted TDG data from a network of sites in the lower Columbia River (https://www.cbr.washington.edu/dart/query/river_graph_text). The network of seven monitoring stations (**Fig. S2**) is operated by the U.S. Army Corps of Engineers, which tracks total dissolved gas (TDG) levels to determine whether TDG levels exceed water quality standards in Oregon; these standards were developed to minimize negative effects on fish physiology. The sites include the John Day navigation lock* and tailwater, The Dalles forebay* and tailwater, Bonneville forebay* and tailwater* (Cascade Island, ~1 km downstream of the Bonneville Dam), and at Warrendale, Oregon, 10 km downstream from Bonneville Dam. Sites denoted with an asterisk operate only from March through September when spill operations are active (https://www.usgs.gov/centers/oregon-water-science-center/science/lower-columbia-river-dissolved-gas-monitoring-network).

TDG sensors placed at Warrendale, Oregon ~10 km downstream of the Bonneville Dam are considered within the tailrace and suitable to capture the supersaturation of gases associated with the dam. The Warrendale site is considered a tailwater sampling site by the USACE; however, Tanner and Bragg (2001) note that some degassing between the spill outflow and Warrendale likely occurs because the sensor is located above the gas compensation depth, which theory suggests is deeper than the river bottom depth at that location. The transit time, *tau* (τ), determined from water velocity, discharge, and the river's cross-sectional area, is approximately 15 h.

We compared TDG data from Warrendale, with TDG data from the USACE monitoring station at Camas, Washington (~40 km downstream of Bonneville Dam), and the two showed similar values throughout the period of our data collection. We considered correcting the *in situ* DO data at the Camas site (SATURN-08) to account for supersaturation effects in dissolved gases (e.g., Roley et al., 2023), but the fact that the sequence of dams in the lower Columbia are relatively close together (i.e., Bonneville, The Dalles, John Day) makes it difficult to disentangle the influence of each dam on oxygen concentrations and saturation. Similarly, correcting the SATURN-08 (Camas) data for spill volume/rate at Bonneville did not significantly improve the estimates of daily GPP, ER, and NEP made without corrections, so we used uncorrected hourly data for our calculations. Error arising from not accounting for gas supersaturation would tend toward underestimation of GPP and overestimation of ER since gases in supersaturated waters will tend to diffuse out into the atmosphere, leading to an underestimation of daily increases in DO. Conversely, ER could be overestimated because the greater tendency for DO to leave a supersaturated solution would produce falsely elevated losses, which would be attributed to ER. Thus, our estimates of NEP

296 could be slightly lower than the true values; however, we believe our calculated rates provide
297 a reasonable approximation of NEP.

298 **Bottle incubations**. Water samples for measurement of DO, nutrients, and chl *a* were
299 collected weekly at noon (±45 min) at both SATURN-06 (Willamette) and SATURN-08
300 (Columbia) at two depths (surface and 1% light level, determined by PAR sensor profile), in
301 triplicate 1 L brown Nalgene bottles using a Van Dorn bottle (WildCo, Saginaw, MI). If the
302 river bottom was shallower than the 1% light level, samples were taken from ~0.5 m above
303 the bottom. Water samples were transported to the laboratory in a cooler on ice (<1 h),
304 transferred into 300 mL BOD bottles (Wheaton®; Wheaton Industries, Inc., Millville, N.J.),
305 and grouped as follows: (1) clear, surface water (n=3); (2) screened, deep water (1% light
306 level; n=3); (3) dark surface water (n=3); and (4) dark deep water (n=3).

307 The groups of bottles were incubated in an environmental chamber at 15°C in the
308 laboratory with full spectrum, "cool-white" lighting (maximum irradiance of 260 µmol
309 photons m^{-2} s^{-1}). The clear bottles were incubated at 100% and 1% of ambient light
310 (measured in light profiles described above), achieved using layers of neutral density
311 screening. Net primary production (NPP) was determined from changes in DO between time
312 zero (T_0) and 4 h, divided by the period of incubation and applied to the number of hours of
313 daylight on the day of sample collection. In order to account for the effect of vertical mixing
314 and its impact on rates of primary production during the day, the NPP measurements from
315 the 100% and 1% laboratory incubations were averaged for comparison with the *in situ* data.
316 NPP rates were adjusted for differences between *in situ* and incubation temperature in the
317 laboratory using a Q10 value of 2 (76).

To determine ER in the absence of photosynthesis, dark bottles (groups 3 and 4) were completely shielded from light under two black garbage bags [measured at <0.5 µmol photons m^{-2} s^{-1}, below the limit at which most phytoplankton can photosynthesize (77)]. All samples were placed in the 15°C environmental chamber on a shaker table (85 rpm) to prevent settling during incubation. DO (in mg L^{-1} and % saturation), temperature, and ambient pressure were measured using a YSI (Yellow Springs Instruments, Yellow Springs, OH) OBOD (Optical Biochemical Oxygen Demand) 626401 probe. The probe was designed to fit snugly in BOD bottles to avoid trapping of gas bubbles. Homogeneous circulation during measurement was achieved using a motorized stirring paddle set on low speed during measurements. After initial measurement (T_0), samples were immediately capped with a glass stopper and sealed with Parafilm™, with care taken to avoid trapping gas bubbles. After 4 h ±20 min, DO was re-measured in each sample (T_{4h}). Respiration rate measurements were adjusted for temperature differences between the environmental chamber and the river using a Q_{10} value of 2.2 (76).

Chlorophyll *a* and nutrients. 100-200 mL of surface and bottom water samples were passed through a GF/F filter (nominal pore size of 0.7 µm) using gentle vacuum pressure (<100 mmHg) and stored at -20°C pending extraction and analysis. Chlorophyll *a* (chl *a*) was extracted from the filters in 90% acetone for 24 h and determined according to the non-acidified method (78) using a Turner Trilogy fluorometer (Turner Designs, Sunnyvale, CA) calibrated with pure chlorophyll a from *Anacystis nidulans* (Sigma-Aldrich Inc., St. Louis, MO). Measurements of chl *a* were used to correct fluorescence data from the *in situ* sensors using regression slope values of 2.99 and 2.17 (with intercepts of 1.11 and 0.74) for the Columbia and Willamette Rivers, respectively.

Duplicate samples were collected into acid-washed 30 or 60 mL polycarbonate (Nalgene, Thermo Fisher Scientific, Inc., Waltham, MA) bottles from the surface and bottom for inorganic nutrient analysis. The samples were filtered through GF/F filters (nominal porosity of 0.7 μm) and stored at -20°C pending analysis. Nitrate, nitrite, ammonium, and ortho-phosphate were measured colorimetrically using an Astoria-Pacific Rapid Flow Analyzer (Astoria-Pacific Inc., Clackamas, OR) (79-81). Laboratory measurements made for samples collected at two depths were averaged and then used to correct the nitrate sensor data, producing slopes of 0.91 and 0.83, and intercepts of -1.88 and -1.11 for the Columbia and Willamette, respectively.

Statistical analysis. Generalized additive modeling (GAM) is a statistical approach used to estimate relationships between response and predictor variables without the assumption of linearity (82, 83). Using the *mgcv* package (v 1.8-9) in R (84, 85) we explored relationships between (1) the light attenuation coefficient (K_d) and environmental variables (river discharge, chlorophyll *a* concentration, and turbidity) in both the Columbia and Willamette Rivers and (2) NEP and environmental variables in both the Columbia and Willamette Rivers with generalized additive models (GAM) that employed the Gaussian method. The number of smooth functions (*s*) was chosen to maximize the percentage of deviance explained by the model and by minimizing generalized cross-validation scores (GCV).

Results

Water quality in the Columbia and Willamette Rivers. River discharge was highest between May 15 and May 29, peaking at ~13,000 m^3 s^{-1} on May 25, 2018 (**Fig. 2**).

Discharge and turbidity were correlated both in the Columbia River ($r = 0.93$; $R^2 = 0.87$; $p < 0.001$) and the Willamette ($r = 0.75$; $R^2 = 0.57$; $p < 0.001$) (not shown). Among our observations, chl *a* values in the Columbia consistently exceeded those in the Willamette, with peak chl *a* concentrations observed in May prior to the spring freshet (May 6, 2018). Once the freshet subsided, chl *a* concentrations in the Columbia increased and remained high through the summer, characterized by episodic peaks. High, episodic peaks in chl *a* were also observed in the Willamette in the summer, with very low values observed during the winter months.

Figure 2. Water quality parameters in the Columbia River at the Port of Camas-Washougal, WA and in the Willamette River in downtown Portland, OR. A) Discharge in the Columbia at Bonneville Dam; B) discharge in the Willamette in downtown Portland at the Morrison Bridge; C) 1% light depth determined at the Port of Camas-Washougal in the Columbia River at Camas, WA; D) 1% light depth determined in the Willamette River near the Morrison Bridge; E) turbidity (NTU) determined in the Columbia River at the Port of Camas-Washougal; F) turbidity (NTU) determined in the Willamette River near Morrison Bridge; E) chlorophyll *a* fluorescence (RFU) determined in the Columbia River at the Port of Camas-Washougal; F) chlorophyll *a* fluorescence determined in the Willamette River at the Morrison Bridge in downtown Portland, OR.

Light penetration depth and attenuation coefficient. In the Columbia 1% light depths ranged from approximately 4–10 m, with the deepest light penetration observed in

January and May (**Fig. 2**); the shallowest 1% light depths coincided with periods of low river discharge. The 1% light depth shoaled to 4–6 m over the course of the spring phytoplankton bloom (mid-April to late June), deepening after the freshet subsided to ~7–7.5 m by late summer. In the Willamette River, the shallowest light penetration depths (1% light level; ~2 m) corresponded with peaks in turbidity and discharge events in the winter and spring (February, March, and April). As flow in the Willamette subsided from May through July, light penetration in the water column increased to ~7.5 m.

Vertical light attenuation coefficient values (K_d) ranged from 0.6–1.1 m^{-1} in the Columbia and 0.6–2.2 m^{-1} in the Willamette, with consistently deeper light penetration depths in the Columbia, particularly in autumn and winter (**Fig. 2**). A generalized additive model (GAM) to predict the light attenuation coefficient, K_d, using turbidity, chlorophyll, and river discharge as smooth terms (**Fig. 3**) yielded only one predictor for the Columbia: turbidity ($p = 0.00021$), which accounted for 91.0% of variation in K_d. In contrast, GAM analysis of factors influencing the light attenuation constant (K_d) in the Willamette identified both turbidity and river discharge as predictors ($p = 0.011$, discharge, $p = 0.00033$, turbidity; 92.1% deviance explained). Turbidity, which depresses primary production as light is attenuated through absorption and scattering (86), was, on average, 25% higher in the Willamette than in the Columbia (calculated as the average of day-for-day percent difference between the two sites). In addition to scattering, pigments like chlorophyll *a* contribute to turbidity and 76.4% of the deviance in turbidity was explained by a combination of river discharge and chlorophyll in the Willamette River, with chlorophyll accounting for only 7.7% of the variation in turbidity ($n = 377$). In the Columbia, 93.7% of variation in turbidity was accounted for by river discharge and chlorophyll, with 43.5% explained by chlorophyll

(n = 247). This difference in the turbidity-chlorophyll relationship between the two rivers indicates that phytoplankton influences light attenuation/absorption in the Columbia more than the Willamette.

Figure 3. Light attenuation coefficient (K_d, in m^{-1}) versus river discharge, chlorophyll *a* concentration, and turbidity. Data in A, C, and E come from the Columbia River at the Port of Camas-Washougal, while B, D, and F come from the Willamette River at the Morrison Bridge in downtown Portland, OR. The line represents output from a Generalized Additive Model describing the relationship between each parameter and K_d.

Vertical profiles of water quality parameters. Profiles of temperature, dissolved oxygen (DO), nitrate, and chlorophyll were vertically homogeneous through the water column, with surface and bottom values of these parameters varying by <1.5% in both the Columbia and the Willamette (**Fig. 4**). Vertical profile data for temperature and DO were collected continuously during up and down casts, while discrete values were determined at the surface and near the bottom for nitrate and chlorophyll *a* concentrations.

Figure 4. Relationships between water quality parameters recorded at the surface and at depth (river bottom) in the Columbia River at Camas, Washington. (A) Temperature (°C); (B) dissolved oxygen percent saturation relative to air (DO%); (C) chlorophyll *a* (µg L^{-1}); (D) nitrate concentration (µM).

GPP, ER, and NEP calculated from *in situ* data. Spill over the Bonneville Dam influences DO and other dissolved gases downstream; therefore, we examined the relationship between spill volume and TDG (total dissolved gas) concentrations during periods of active spill. In 2017-2018, there were several periods of active spill over Bonneville Dam (**Fig. S3**), including during the summer of 2017 (7/1/172-9/1/17), a short period in February 2018 (2/5/18-2/20/18), a period in April that reflected the onset and development of the spring freshet (beginning on ~4/12/18 and peaking on 5/18/18; subsiding on 6/15/18). Because Bonneville is a run-of-the-river dam, spill occurs due to high water volumes (passive) as well as active spill; active spill took place between 6/15/18 and the end of our time series in July 2018.

The relationship between spill volume and TDG saturation differed with the magnitude of flow in three distinct regression segments: (1) at spill volumes <40 kcfs, there is no relationship between spill and TDG pressure or saturation; (2) for spill volumes between 60 and 150 kcfs, TDG saturation is predicted from $y = 0.1374x + 102.65$ ($R^2 = 0.8878$), where y is TDG saturation and x is spill volume; (3) at spill volumes >150 kcfs, the relationship is described by $y = 0.0416x + 115.8$, $R^2 = 0.8333$. The Columbia River site at Camas-Washougal, WA is located approximately 40 km downstream of Bonneville Dam, 108 km downstream of The Dalles dam and 148 km downstream of the John Day dam. As evidenced by the persistent supersaturation of dissolved gases relative to the atmosphere in the forebays and tailwater sites at Bonneville Dam, The Dalles Dam, and John Day Dam (i.e., upstream of the dam; see https://www.nwd-wc.usace.army.mil/ftppub/water_quality/tdg/ for data tables), the distance between dams is not great enough for the spill-driven gas supersaturation to reach equilibrium with the atmosphere and DO in this extensive stretch of

456 the river is always supersaturated. However, the daily ranges in dissolved oxygen
457 concentration and percent saturation were similar during periods associated with spill and
458 after the spill ceases (i.e., September 1), which indicates that diel patterns reflect biological
459 activity and not dam operations. Daily changes in DO persisted regardless of river discharge
460 volume, suggesting a biological signal (**Fig. S4**).

461 With the assumption that daily changes in DO reflect biological activity, we
462 calculated GPP and ER using sensor data. *In situ* GPP showed strong seasonality, with the
463 highest values observed in the summer months at both the Columbia River site and in the
464 Willamette River (**Fig. 5**). There was a dip in GPP values associated with spring freshet
465 flows in the Columbia River that was not seen in the Willamette. The timing of the local
466 minimum in GPP coincided with that of strong flows associated with snowmelt, consistent
467 with a dilution effect.

468

469 **Figure 5. Comparison of NEM, GPP, and ER between the Columbia and Willamette**
470 **rivers. (A) daily GPP, NEM, and ER for the Columbia River at Camas-Washougal WA,**
471 **calculated using data from the SATURN-08 sensor. (B) daily GPP, NEM, and ER for**
472 **the Willamette River at Willamette Park OR, calculated using data from the SATURN-**
473 **06 sensor.**

474

475 With the exception of a few observations in September and October, daily *in situ* GPP
476 exceeded *in situ* ER in the Columbia, resulting in slightly positive daily NEP values (**Fig. 5**).
477 Between March and May when GPP was highest, ER was also at its peak, dampening NPP
478 and producing NEP values close to zero. Although there was a gap in sensor data between

October and February, observations made just before and after the gap suggest that both production and respiration were low during winter, and this is consistent with low chl *a* concentrations and algal densities observed during the winter in the system (87). The daily NEP values averaged 0.42 gC m^{-2} d^{-1} for the 249 days where data were collected; if we assume that the missing 128 winter days from the period (Oct 2 and February 7) had NEP values similar to the period of February 7-14 when there were data available (average = 0.17 gC m^{-2} d^{-1}), then an estimate for annual NEP in the Columbia would be 121.30 gC m^{-2} y^{-1}:

$$NEP_{annual} = (0.17 \text{ gC } m^{-2} d^{-1}) * 128 \text{ d} + (0.42 \text{ gC } m^{-2} d^{-1}) * 237 \text{ d} = 121.3 \text{ gC } m^{-2} y^{-1}$$

The Willamette River had lower overall NEP than the Columbia, with slightly negative daily values observed between June and August, indicating net heterotrophy (88). GPP values in the Willamette were high during the summer months, but were nearly matched by high ER, leading to NEP values that were generally close to zero. Annual NEP in the Willamette River was -16.67 gC m^{-2} y^{-1};. Note that the *in situ* data included some daily ER rates that were positive; these data were removed from the calculated estimate since positive respiration rates are impossible.

Hourly rates of change in DO in the Willamette were more variable than in the Columbia in the spring and summer months, where the summer was characterized by low discharge, high temperatures, lower turbidity, and deeper 1% light depths. Summer conditions include large cyanobacteria blooms in Ross Island Lagoon (Oregon Department of Environmental Quality). Slower growth (production and respiration) in the winter months led to small hourly differences in DO in both systems and low GPP, ER, and NEP values.

In both the Columbia and Willamette Rivers, ER and GPP were coupled according to *in situ* observations (**Fig. 6**), as has been observed elsewhere (13). The relationships are described by the linear equations $y = -0.84x + 0.044$, $R^2 = 0.804$ for the Columbia and $y = -0.90x + 0.054$, $R^2 = 0.868$ for the Willamette, where y is ER and x is GPP. In both rivers, GPP and ER increased with temperature to a maximum (ER rates became more negative with increasing temperature, interpreted as an increase in ER).

Figure 6. Relationships between primary production and respiration in the Columbia (left panels) and Willamette (right panels) Rivers. A) Ecosystem Respiration (ER) versus Gross Primary Production (GPP) determined using continuous *in situ* sensors in the Columbia River; B) ER vs. GPP determined using continuous *in situ* sensors in the Willamette River; C) respiration (R) versus net primary production (GPP) determined in bottle incubations in the Columbia River; D) R vs. GPP determined in bottle incubations in the Willamette River; E) GPP or ER versus temperature in the Columbia River determined using in situ sensors; F) GPP or ER versus temperature in the Willamette River determined using in situ sensors; R or NPP versus temperature in the Columbia River determined in bottle incubations; R or NPP in the Willamette River determined in bottle incubations.

GPP, ER, and NEP calculated from bottle incubation data. In contrast to *in situ*, the relationships between GPP and ER in the Columbia and Willamette Rivers were non-linear, with the highest ER values occurring when GPP levels were moderate (**Fig. 6**).

GAM analysis of relationships between GPP and ER with water quality parameters showed that variations in both GPP and ER could be explained by temperature, and that seasonal discharge patterns in the Columbia influenced GPP and ER, but not in the Willamette (**Figs. 7, 8**). There was a weak relationship with instream chlorophyll concentration in both rivers.

Figure 7. Gross Primary Production (GPP) versus water quality parameters [river discharge, chlorophyll *a* (Chl), and temperature for the Columbia (left panels) and the Willamette (right panels)]. The line represents a Generalized Additive Model showing relationships between GPP and environmental variables.

Figure 8. Ecosystem Respiration (ER) versus water quality parameters [river discharge, chlorophyll *a* (Chl), and temperature for the Columbia (left panels) and the Willamette (right panels)]. The line represents a Generalized Additive Model showing relationships between GPP and environmental variables.

A comparison of GPP calculated from in situ and bottle data showed that departures from a 1:1 line varied with season or river conditions (**Fig. 9**). There were only small differences between the bottle and *in situ* measurements in the Columbia in the winter; in May and June, when river discharge volumes were highest, GPP measured in bottle incubations were lower than *in situ* measurements, suggesting that primary production is driven by larger ecosystem processes not captured in water samples (i.e., vascular plants, including submerged aquatic vegetation and riparian plant communities). In the early spring

and summer, however, GPP determined in the bottle incubations exceeded that determined from *in situ* sensor data, suggesting that phytoplankton-associated primary production is a significant contributor to ecosystem primary production.

Figure 9. GPP determined using *in situ* sensor data versus GPP determined using bottle incubations (R and NPP). A 1:1 would be expected if measurements were the same using both techniques. Superimposed on the graph is an indication of seasonal affiliation of data points to illustrate the hypothesis that bottle incubations exhibit higher productivity than *in situ* rates during the spring and summer months when river discharge volumes are relatively low, while *in situ* GPP exceeds that determined in bottle incubations during the spring freshet when water levels are high. We hypothesize that a comparison of GPP determined from *in situ* observations and bottle incubations can be used to identify time periods when GPP in the river is dominated by instream phytoplankton production vs. vascular plants.

In contrast to the Columbia, NPP and GPP rates determined in bottle incubations from the Willamette were almost always lower than the *in situ* measurements, suggesting that bottle incubations underestimate primary production.

Discussion

Large rivers are globally significant, highly complex systems. As important landscape integrators (89, 90), they influence global carbon and material budgets, provide crucial habitat for myriad species, including threatened and vulnerable taxa, and contribute key

ecosystem services (32, 38, 91). The Columbia and Willamette Rivers are both large U.S. rivers with strong variations in modern, historical, and predicted future flows (92-94) (95); each makes important contributions to the region's economy, supports critical ecosystems (9), and has been heavily impacted by human activities, including a changing climate (96), similar to rivers worldwide (97).

Aside from high primary production observed within impoundments (Bristow et al. 1985), most rivers are considered net sources of CO_2 (Butman and Raymond 2011) and are among the most heterotrophic systems on Earth (98). Yet, in many ways, large rivers – particularly those characterized by flow interruptions associated with dams – do not behave like their smaller counterparts (13). For example, GPP and ER have been shown to increase along with mean discharge (Q) in smaller rivers, up to a threshold of ~10 $m^3 s^{-1}$ (99); however, the flow volumes in the Columbia and Willamette far exceed these levels, making comparisons difficult. Previous work in the Columbia's Hanford Reach downstream of Priest Rapids dam showed that there was no relationship between Q and GPP (13); in contrast, Q accounted for 44.1% of variation in GPP and 39.8% of variation in ER in the Columbia in this study, with no relationship between Q and NEP. Q did not predict GPP, ER, or NEP in the Willamette River. The highest GPP, ER, NEP, and chlorophyll concentrations in the Columbia were observed just prior to the spring freshet in early May, when Q was ~5000 $m^3 s^{-1}$. This pre-freshet period is characterized by strong phytoplankton growth, dominated by large diatoms, including *Asterionella formosa* and *Aulacoseira* spp. (87, 100, 101), both species commonly found in large rivers worldwide [e.g., the Murray River in Australia (102)].

While the global average NEP for temperate rivers is -260 g C m^{-2} y^{-1} (29), NEP was net positive in both the Columbia (121.30 g C m^{-2} y^{-1}) and slightly negative in the Willamette (-18.8 gC m^{-2} y^{-1}). While these annual rates include assumptions, particularly around missing data in the winter months at the Columbia site, the daily NEP values suggest that, on the whole, these rivers are close to neutral, which supports the idea that they are not highly heterotrophic systems.

The deeper depths of large rivers beg the question: are there vertical discontinuities, or stratification that limit the utility of single-depth measurements? Weekly vertical profiles of water quality parameters showed that DO and other environmental parameters (temperature, inorganic nutrients, chlorophyll *a*) were vertically uniform in both rivers across seasons, indicating not only that measurements made at a single depth reasonably approximate the water column, but that constituents contained therein, including phytoplankton, likely reach the benthos, with implications for carbon and nutrient cycling between the water column and sediments (103, 104). This interaction provides a mechanism by which pelagic primary production can fuel benthic food webs, including prey taxa that support juvenile salmon, namely amphipods (Order Amphipoda) and benthic chironomids (105).

Similar to observations by Roley et al. (13), GPP and ER were coupled in the Columbia and in the Willamette according to data from *in situ* DO sensors. However, the relationship between respiration (R) and net primary production (NPP) in the bottle incubations varied in a non-linear way that is consistent with seasonal effects (**Fig. 8**). That is, at low GPP, there is a linear relationship between ER and GPP to a maximum; at high GPP, values of ER are low. This likely reflects the metabolism of different organic matter

615 sources (autochthonous vs. autochthonous), with relatively high rates of ER during months of
616 the year when GPP is low and allochthonous organic carbon provides the main substrate for
617 respiration. During periods of low primary production, for example in the winter, metabolism
618 by heterotrophs likely makes a greater proportional contribution to respiration than in the
619 spring and summer when primary producers are more abundant (106). As autochthonous
620 primary production increases, the ratio of GPP:ER increases; the ratio of photosynthesis to
621 respiration in phytoplankton can be more than 50, as shown in laboratory cultures (107, 108).
622 In addition to seasonal variation in the relationship between GPP and R in the bottle
623 incubations, we observed seasonality in differences between *in situ* GPP and GPP determined
624 using bottle incubations. During low-flow periods, laboratory measurements suggest higher
625 primary production compared to the *in situ* observations, while during periods of high flow in
626 the late spring, GPP is underestimated in the laboratory incubations compared to the *in situ*
627 observations. More broadly, an underestimation of GPP in the continuous, *in situ* data, and an
628 overestimation of ER is consistent with the effect of gas supersaturation associated with dam
629 operations (75); gases in supersaturated waters will tend to diffuse into the atmosphere,
630 leading to an underestimation of GPP computed from hourly change in DO. Conversely, ER
631 could be overestimated under conditions where gases are supersaturated; since DO has a
632 greater tendency to leave a supersaturated solution, the observed losses -- attributed to ER
633 when using *in situ* data – would reflect a combination of ER plus loss to the atmosphere
634 enhanced by the supersaturation. It is not uncommon for differences to be observed between
635 *in situ* and *in vitro* data (109), often attributed to so-called 'bottle effects' (110), where the
636 suppression of mixing and overturn can lead to higher apparent respiration rates. In the

637 present study, gas supersaturation provides a mechanistic explanation for observed
638 differences.

639 At the landscape scale, positive NEP in the lower Columbia River leads to delivery of
640 organic matter to the estuary, where it undergoes chemical transformation in the estuarine
641 turbidity maximum (111, 112), effectively shifting primary production away from tidal
642 freshwater habitats and into estuarine food webs. Within tidal freshwater habitats, longer
643 residence times and lower discharge volumes allow for the build-up of phytoplankton
644 standing stocks; transformation of organic carbon can occur via grazing (113-115) or by the
645 re-packaging of phytoplankton organic carbon into more labile forms by infection of fungal
646 parasites known as chytrids (116). A study by Maier and Peterson (117) suggested that losses
647 to microbial parasitism of the dominant primary producers during the spring blooms could
648 rival grazing impacts. Although the degree to which phytoplankton contributes to river food
649 webs, including juvenile salmonids, remains unclear, phytoplankton-derived organic matter
650 may complement alternative sources of primary production derived from macro-detritus from
651 the region's wetlands (7, 9).

652 GPP in the Columbia was lower than in the Willamette during the summer months.
653 Yet, because ER rates were also higher in the Willamette, NEP was generally weakly
654 negative throughout the study, with moderately negative values observed during the period of
655 greatest GPP. While both rivers had chlorophyll concentrations that are lower than would be
656 expected in eutrophic systems (28), the larger range in GPP and ER in the Willamette suggest
657 that this river shows more eutrophic tendencies than the Columbia, consistent with higher
658 nutrient loads (118). A combination of lower biological drawdown and high agricultural
659 inputs make inorganic nutrient loads in the Willamette higher than the Columbia (51, 118).

660 The seasonal shift from negative to positive NEP in the Willamette is similar to the pattern
661 observed in a modeling study of the river Thames, in which the river is autotrophic during
662 low-flow periods (spring and early summer) but heterotrophic during higher-flow periods
663 (119).

664 We investigated K_d and light penetration depth to explore the importance of light
665 limitation in these two large rivers. Light penetration depth (Z_{eu}) was greater in the Columbia
666 than in the Willamette, consistent with differences between "green" and "brown" rivers and
667 supporting the idea that primary production is light-limited in the Willamette River (66). The
668 estimated K_d values in this study ranged from 0.6–1.1 and 0.6–2.2 for the Columbia and
669 Willamette, respectively; the largest K_d values here are similar to those calculated for filtered
670 seawater, which range from 1.03 to 2.7 m^{-1} (120), demonstrating the range of water clarity
671 observed during different seasons and conditions. The observation that high river discharge
672 coincides with the shallowest Z_{eu} in the Willamette River, but the deepest Z_{eu} in the
673 Columbia, highlights the different relationship between discharge and turbidity in the two
674 rivers; there is higher turbidity per unit volume of the Willamette, leading to an influx of
675 particles at high discharge, while in the Columbia, the snowpack-driven flows – which tend
676 to be relatively clear – have lower turbidity per unit volume, making periods of high flow
677 ones of greater water clarity in the Columbia. With chlorophyll accounting for <10% of
678 turbidity variation, it is unlikely that differences in the specific absorption of light by
679 different phytoplankton taxa (121) influenced K_d in the Willamette River, a water body
680 characterized by high turbidity (122). However, in the Columbia, chlorophyll variability
681 accounted for ~40% of deviance in turbidity, suggesting that phytoplankton contribute to
682 light absorption.

683 We did not investigate along-stream variability in water quality parameters, which
684 could have been achieved through a two-station approach; a two station approach was not
685 practical for the same reasons outlined in Roley et al. (13). In addition, previous work
686 showed that fluorescent dissolved organic matter and dissolved organic carbon exhibit only
687 small daily variations in a synoptic survey of the lower Columbia River below Bonneville
688 Dam (123). Prahl et al. (66) showed that increases in chlorophyll concentration between
689 Bonneville Dam and the mouth of the Columbia River estuary were attributable to steady,
690 autochthonous growth rather than to external inputs of primary production. A progressive,
691 along-stream increase in the build-up of phytoplankton biomass is consistent with low
692 synoptic variability in riverine conditions, supporting the applicability of data from *in situ*
693 sensors for determination of NEM, GPP, and ER in these river systems using a single-station
694 approach. Further, (Bernhardt et al. 2022) point out that the dominant controls on primary
695 production and respiration vary at scales that encompass large stretches of the river (e.g.,
696 light level, nutrient concentration, precipitation, phytoplankton standing stocks; (124). In
697 addition, Roley et al. concluded that a single-station approach was adequate for calculation of
698 NEP in the Columbia River at a site downstream of Priest Rapids dam; in that study,
699 simultaneous measurements of argon and dissolved oxygen were used to decipher the
700 biological component of gas fluxes used in calculations of hourly variation in DO for
701 determination of GPP, ER, and NEP. Therefore, it is likely that a one-station approach is
702 sufficient to approximate NEP in the lower stretches of the Columbia and Willamette.
703 However, we acknowledge that our NEP estimates could be influenced by the fact that we
704 are not re-sampling the same water during the day and night.
705

Conclusions

In this study, we showed that unlike most rivers worldwide, annual net ecosystem production in the Columbia River is positive and while annual NEP in the Willamette River is negative, values are much smaller than in many other systems. A comparison between *in situ* data and bottle incubations supports a hypothesis that during periods of high river discharge, ecosystem primary production exceeds instream primary production, while during periods of lower flow and water elevation, instream primary production is an important contributor to ecosystem production. In addition, seasonal differences in the relationship between respiration and GPP in bottle incubations suggest that during periods characterized by low GPP, respiration is driven by allochthonous organic matter, while during periods associated with high GPP, respiration is driven by autochthonous organic matter. Observations of positive NEP during most of the year—indicating net production of organic carbon in the system—are consistent with the idea that the Columbia is a "green" river that supports net growth of pelagic phytoplankton. In a green river, GPP exceeds respiration, resulting in an accumulation of organic matter that can contribute to pelagic food webs, export particulate organic carbon to the sea, and fuel bacterial secondary production in the estuary. We conclude with a hypothesis that vascular plants (either submerged or in riparian areas that are inundated at tidal scales) dominate aquatic ecosystem primary production during high-flow periods associated with the spring freshet, as well in the winter season, while instream phytoplankton dominate aquatic ecosystem primary production during the spring bloom and summer.

Acknowledgments

This work was funded by Bonneville Power Administration administered by the Lower Columbia Estuary Partnership (BPA Project Number 2003-007-00). We thank the Ecosystem Monitoring Program team for valuable discussions about salmon habitat and river restoration and acknowledge the critical insights of Dr. Fred Prahl of Oregon State University that informed our work on Columbia and Willamette River biogeochemistry as part of the National Science Foundation's Science and Technology Center for Coastal Margin Observation and Prediction (award OCE-0424602).

References

1. Field C, Behrenfeld M, Randerson J. Primary production of the biosphere: Integrating terrestrial and oceanic components. Science. 1998;281:237-41.
2. Falkowski P, Scholes RJ, Boyle E, Canadell J, Canfield D, Elser J, et al. The global carbon cycle: A test of our knowledge of Earth as a system. Science. 2000;290:291-6.
3. Cole JJ, Prairie YT, Caraco NF, McDowell WH, Tranvik LJ, Striegl RG, et al. Plumbing the global carbon cycle: Integrating inland waters into the terrestrial carbon budget. Ecosystems. 2007;10:171-84.
4. Alin S, Siedlecki S, Hales B, Mathis J, Evans W, Stukel M, et al. Coastal carbon synthesis for the continental shelf of the North American Pacific Coast (NAPC): Preliminary results. Ocean Carbon and Biogeochemistry News. 2012;5:1-5.
5. Donner SD, Scavia D. How climate controls the flux of nitrogen by the Mississippi River and the development of hypoxia in the Gulf of Mexico. . Limnology & Oceanography. 2007;52:856-61.
6. Howarth R, Chan F, Conley DJ, Garnier J, Doney SC, Marino R, et al. Coupled biogeochemical cycles: Eutrophication and hypoxia in temperate estuaries and coastal marine ecosystems. Front Ecol Environ. 2011;9:18-26.
7. Weitkamp LA. A review of the effects of dams on the Columbia River estuarine environment, with special reference to salmonids. Portland, Oregon; 1994. Contract No.: Contract 227 DE_A179-93BP99021.
8. Pauly D, Christensen V. Primary production required to sustain global fisheries. Nature. 1995;374:255-7.
9. Bottom D, Simenstad CA, Burke J, Baptista AM, Jay DA, Jones KK, et al. Salmon at river's end: the role of the estuary in the decline and recovery of Collumbia River salmon. Seattle, WA: National Marine Fisheries Service; 2005. Contract No.: NMFS-NWFSC-68.
10. Peipoch M, Ensign SH. Deciphering the origin of riverine phytoplankton using in situ chlorophyll sensors. Limnology and Oceanography Letters. 2022;7:159-66.
11. Roberts BJ, Mulholland PJ, Hill WR. Multiple scales of temporal variability in ecosystem metabolism rates: Results from 2 years of continuous monitoring in a forested headwater stream. Ecosystems. 2007;10:588-606.
12. Bauer JE, Cai W-J, Raymond PA, Bianchi TS, Hopkinson CS, Regnier PAG. The changing carbon cycle of the coastal ocean. Nature. 2013;504:61-70.
13. Roley SS, Hall ROJ, Perkins W, Garayburu-Caruso VA, Stegen JC. Coupled primary production and respiration in a large river contrasts with smaller rivers and streams. Limnology & Oceanography. 2023;68(11):2461-75.
14. Baker DJ, Schmitt RW, Wunsch C. Endowments and new institutions for long-term observations. Oceanography. 2007;20:10-4.
15. Agis M, Granda A, Dolan JR. A cautionary note: examples of possible microbial community dynamics in dilution grazing experiments. . J Exp Mar Biol Ecol. 2007;341:176-83.
16. Johnson KS, Needoba JA, Riser SC, Showers WJ. Chemical sensor networks for the aquatic environment. Chemical Reviews. 2007;107(2):623-40.
17. Meinson P, Idrizaj A, Noges P, Noges T, Laas A. Continuous and high-frequency measurements in limnology: history, applications, and future challenges. Environmental Reviews. 2016;24(1):52-62.
18. Pellerin BA, Bergamaschi BA, Murdoch PS, Downing BD, Saraceno JF, Aiken GR, et al. The aquatic real-time monitoring network; in-situ optical sensors for monitoring the nation's water quality. US Geological Survey Fact Sheet 2011:2.
19. Savoy P, Appling AP, Heffernan JB, Stets EG, Read JS, Harvey JW, et al. Metabolic rhythms in flowing waters: An approach for classifying river productivity regimes. Limnology & Oceanography. 2019;64(5):1835-51.

20. Gilbert M, Needoba J, Koch C, Barnard A, Baptista A. Nutrient loading and transformations in the Columbia River Estuary determined by high-resolution in situ sensors. Estuaries and Coasts. 2013;36:708-27.
21. Lloyd CEM, Freer E, Joohnes PJ, Collins AL. Using hysteresis analysis of high-resolution water quality monitoring data, including uncertainty, to infer controls on nutrient and sediment transfer in catchments. Science of the Total Environment. 2016;543:388-404.
22. Caffrey JM. Production, respiration and net ecosystem metabolism in U.S. estuaries. Environmental Monitoring and Assessment. 2003;81:207-19.
23. Odum HT. Primary production in flowing waters. Limnology & Oceanography. 1956;1:102-17.
24. Swaney DP, Howarth RW, Butler TJ. A novel approach for estimating ecosystem production and respiration in estuaries: Application to the oligohaline and mesohaline Hudson River. Limnology and Oceanography. 1999;44:1509-21.
25. Needoba J, Peterson T, Johnson K. Method for the quantification of aquatic primary production and net ecosystem metabolism using in situ dissolved oxygen sensors. . In: Tiquia-Arashiro S, editor. Molecular biological technologies for ocean sensing. Totowa, NJ: Humana Press.; 2012.
26. Staehr P, Bade D, Koch G, Williamson C, Hanson P, Cole J, et al. Lake metabolism and the diel oxygen technique: State of the science. Limnology & Oceanography: Methods. 2010;8:628-44.
27. O'Sullivan PE. Eutrophication. International Journal of Environmental Studies. 1994;47(3-4):173-95.
28. Nixon SW. Coastal marine eutrophication - A definition, social causes, and future concerns. Ophelia. 1995;41(1):199-219.
29. Battin TJ, Lauerwald R, Bernhardt ES, Bertuzzo E, Gómez Gener L, Hall Jr. RO, et al. River ecosystem metabolism and carbon biogeochemistry in a changing world. Nature. 2023;613:449-59.
30. Appling AP, Read JS, Winslow LA, Arroita M, Bernhardt ES, Griffiths NA, et al. The metabolic regimes of 356 rivers in the United States. Sci Data. 2018;5:180292.
31. Rinella FA, Janet ML. Seasonal and spatial variability of nutrients and pesticides in streams of the Willamette Basin, Oregon, 1993-95. U.S. Geological Survey; 1998.
32. Naiman RJ. Socio-ecological complexity and the restoration of river ecosystems. Inland Waters. 2013;3(4):391-410.
33. Katz SL, Barnas K, Hicks R, Cowen J, Jenkinson R. Freshwater habitat restoration actions in the Pacific Northwest: a decade's investment in habitat improvement. . Restoration Ecology. 2007;15:494-505.
34. Bilby RE, Currens KP, Fresh KL, Booth DB, Fuerstenberg RR, Lucchetti GL. Why aren't salmon responding to habitat restoration? Fisheries. 2024;49(1):1-48.
35. Beechie TJ, Bolton S. An approach to restoring salmonid habitat-forming processes in Pacific Northwest watersheds. . Fisheries. 1999;24(4):6-15.
36. Acreman MC, Overton IC, King J, Wood PJ, Cowx IG, Dunbar MJ, et al. The changing role of ecohydrological science in guiding environmental flows. Hydrological Sciences Journal. 2014;59(3-4):433-50.
37. Bellmore JR, Benjamin JR, Newsom M, Bountry JA, Dombroski D. Incorporating food web dynamics into ecological restoration: a modeling approach for river ecosystems. Ecological Applications. 2017;27(3):814-32.
38. Naiman RJ, Alldredge JR, Beauchamp DA, Bisson PA, Congleton J, Henny CJ, et al. Developing a broader scientific foundation for river restoration: Columbia River food webs. Proceedings of the National Academy of Sciences of the United States of America. 2012;109(52).
39. Battin TJ, Wiley MW, Ruckelshaus MH, Palmer RN, Korb E, Bartz KK, et al. Projected impacts of climate change on salmon habitat restoration. Proceedings of the National Academy of Sciences. 2007;104(16):6720.

839 40. Beechie T, Imaki H, Greene J, Wade A, Wu H, Pess G, et al. Restoring salmon habitat for a
840 changing climate. River Research and Applications. 2013;29(8):939-60.
841 41. Mũnoz NJ, Reynolds JD, Moore JW, Neff BD. Salmon in clear and present danger. Science.
842 2020;366:582.
843 42. Bank MS, Sonne C, Hansson SV, Rillig MC. Science-informed salmon conservation
844 strategies. Science. 2021;374:700.
845 43. Dauble DD, Hanrahan TP, Geist DR, Parsley MJ. Impacts of the Columbia River
846 Hydroelectric System on Main-Stem Habitats of Fall Chinook Salmon. North American Journal of
847 Fisheries Management. 2003;23(3):641-59.
848 44. Maavara T, Chen Q, Van Meter K, Brown LE, Zhang J, Ni J, et al. River dam impacts on
849 biogeochemical cycling Nat Rev Earth Environ. 2020;1:103-16.
850 45. Maavara T, Lauerwald R, Regnier P, Cappellen PV. Global perturbation of organic carbon
851 cycling by river damming. Nat Commun. 2017;8:15347.
852 46. Waples RS, Zabel RW, Scheuerell MD, Sanderson BL. Evolutionary responses to major
853 anthropogenic changes to their ecosystems: Pacific salmon in the Columbia River hydropower
854 system. Molecular Ecology. 2007;17:84-96.
855 47. Naik PK, Jay DA. Human and climate impacts on Columbia River hydrology and salmonids.
856 River Research and Applications. 2011;27:1270-6.
857 48. Hinrichsen R, Hasselman DJ, Ebbesmeyer C, Shields BA. The Role of Impoundments,
858 Temperature, and Discharge on Colonization of the Columbia River Basin, USA, by Nonindigenous
859 American Shad. Transactions of the American Fisheries Society. 2013;142:887-900.
860 49. Pradeep KN, Jay DA. Estimation of Columbia River virgin flow: 1879 to 1928. Hydrological
861 Processes. 2005;19:1807-24.
862 50. Sherwood CR, Jay DA, Harvey RB, Hamilton P, Simenstad CA. Historical Changes in the
863 Columbia River Estuary. Progress in Oceanography. 1990;25:299-357.
864 51. Sullivan BE, Prahl FG, Small LF, Covert PA. Seasonality of phytoplankton production in the
865 Columbia River: A natural or anthropogenic pattern? . Geochimica Cosmochimica Acta.
866 2001;65:1125-39.
867 52. Maier GO, Simenstad CA. The role of marsh-derived macrodetritus to the food webs of
868 juvenile chinook salmon in a large altered estuary. Estuaries and Coasts. 2009;32:984-98.
869 53. Hall ROJ, Yackulic CB, Kennedy TA, Yard MD, Rosi-Marshall EJ, Voichick N, et al.
870 Turbidity, light, temperature, and hydropeaking control primary productivity in the Colorado River,
871 Grand Canyon. Limnol Oceanogr. 2015;60:512-26.
872 54. Prahl FG, Small LR, Sullivan BA, Cordell J, Simenstad CA, Crump BC, et al.
873 Biogeochemical gradients in the lower Columbia River. Hydrobiologia. 1997;361:37-52.
874 55. Mendonça R, Müller RA, Clow D, Verpoorter C, Raymond P, Tranvik LJ, et al. Organic
875 carbon burial in global lakes and reservoirs. Nat Commun. 2017;8:1694-7.
876 56. Deemer BR, Harrison JA, Li S, Beaulieu JJ, DelSontro T, Barros N, et al. Greenhouse gas
877 emissions from reservoir water surfaces: a new global synthesis. Bioscience. 2016;66:949-64.
878 57. Cooper AR, Infante DM, Daniel WM, Wehrly KE, Wang L, Brenden TO. Assessment of dam
879 effects on streams and fish assemblages of the conterminous USA. Science of the Total Environment.
880 2017;586:879-89.
881 58. Lawrence ER, Kuparinen A, Hutchings JA. Influence of dams on population persistence in
882 Atlantic salmon (Salmo salar). Canadian Journal of Fisheries and Aquatic Sciences. 2016;94(5):329-
883 38.
884 59. Nehlsen W, Williams JE, Lichatowich JA. Pacific salmon at the crossroads: stocks at risk
885 from California, Oregon, Idaho, and Washington. Fisheries. 1991;16(2):4-21.
886 60. McClure MM, Holmes EE, Sanderson BL, Jordan CE. A large-scale, multispecies sta-tus
887 assessment: anadromous salmonids in the Co-lumbia River basin. Ecological Applications.
888 2003;13(4):964-89.

61. Harnish RA, Sharma R, McMichael GA, Langshaw RB, Pearsons TN. Effect of hydroelectric dam operations on the freshwater productivity of a Columbia River fall Chinook salmon population. Canadian Journal of Fisheries and Aquatic Sciences. 2014;71:602-15.
62. Thorp JH, Delong MD. The riverine productivity model — An heuristic view of carbon-sources and organic-processing in large river ecosystems. Oikos. 1994;70:305-8.
63. Thorp JH, Thoms MC, Delong MD. The riverine ecosystem synthesis: Biocomplexity in river networks across space and time. River Research and Applications. 2006;22:123-47.
64. Collie J, Saila S, Walters C, Carpenter S. Of salmon and dams. Science. 2000;290:933-4.
65. Mann CC, Plummer ML. Response to 'Of salmon and dams' by Collie et al. Science. 2000;290:934.
66. Prahl FG, Small LF, Sullivan BA, Cordell J, Simenstad CA, Crump BC, et al. Biogeochemical gradients in the lower Columbia River. Hydrobiologia. 1997;361:37-52.
67. Mulvey M, Leferink R, Borisenko A. Willamette basin rivers & streams assessment. Hillsoro, OR: Oregon Watershed Enhancement Board; 2009.
68. Kammerer JC. Largest Rivers in the United States. Department of the Interior; 1990. Contract No.: Report 87-242.
69. Baptista AM, Seaton C, Wilkin MP, Riseman SF, Needoba JA, Maier D, et al. Infrastructure for collaborative science and societal applications in the Columbia River estuary. Frontiers in Earth Science. 2015;9(4):659-82.
70. Meyer JL, Edwards RT. Ecosystem metabolism and turnover of organic carbon along a blackwater river continuum. Ecology. 1990;7:668-77.
71. Young RG, Huryn AD. Interannual variation in discharge controls ecosystem metabolism along a grassland river continuum. Canadian Journal of Fisheries and Aquatic Sciences. 1996;53:2199-211.
72. Wanninkhof R. Relationship between wind speed and gas exchange over the ocean. Journal of Geophysical Research. 1992;97:7373-82.
73. Wanninkhof R. Relationship between wind speed and gas exchange over the ocean revisited. Limnol Oceangr: Methods. 2014;12:351-62.
74. Bott TL. Primary productivity and community respiration. In: Hauer FR, Lamberti GA, editors. Methods in Stream Ecology, . Paris: Academic Press; 2006. p. 663-90.
75. Li P, Zhu DZ, Li R, Wang Y, Crossman JA, Kuhn WL. Production of total dissolved gas supersaturation at hydropower facilities and its transport: A review. Water Research. 2022;223:119012.
76. Apple JK, Del Giorgio PA, Kemp WM. Temperature regulation of bacterial production, respiration, and growth efficiency in a temperate salt-marsh estuary. . Aquat Microb Ecol. 2006;43:243-54.
77. Peterson DH, Perry MJ, Bencal KE, Talbot MC. Phytoplankton productivity in relation to light intensity: A simple equation. Estuar Coast Shelf Sci. 1987;24:813-32.
78. Welschmeyer NA. Fluorometric analysis of chlorophyll a in the presence of chlorophyll b and pheopigments. Limnology & Oceanography. 1994;39:1985-92.
79. Armstrong FA, Stearns CR, Strickland JD. The measurement of upwelling and subsequent biological processes by means of the Technicon Autoanalyzer® and associated equipment. Deep Sea Research. 1967;14:381-9.
80. APHA, AWWA, WEF. Standard methods for examination of water and wastewater. Washington, D.C. USA; 1992.
81. Holmes RM, Aminot A, Kérouel R, Hooker BA, Peterson BJ. A simple and precise method for measuring ammonium in marine and freshwater ecosystems. Canadian Journal of Fisheries and Aquatic Sciences. 1999;56:1801-8.
82. Hastie T, Tibshirani R. Generalized additive models. New York: Taylor & Francis; 1990. 496 p.

939 83. Wood S. Generalized additive models: an introduction with R. . 2nd ed. Boco Raton: CRC
940 Press; 2017.
941 84. Wood SN. Fast Stable Restricted Maximum Likelihood and Marginal Likelihood Estimation
942 of Semiparametric Generalized Linear Models. Journal of the Royal Statistical Society Series B:
943 Statistical Methodology. 2011;73(1):3-36.
944 85. Pedersen EJ, Miller DL, Simpson GL, Ross N. Hierarchical generalized additive models in
945 ecology: an introduction with mgcv. PeerJ. 2019;7:e6876.
946 86. Cloern JE. Turbidity as a control on phytoplank-ton biomass and productivity in estuaries.
947 ContinentalShelf Research. 1987;7:1367–81.
948 87. Maier MA. Ecology of diatoms and their fungal parasites in the Columbia River: Oregon
949 Health & Science University; 2014.
950 88. Hopkinson CS. Shallow-water benthic and pelagic metabolism: Evidence of heterotrophy in
951 the nearshore Georgia Bight. Marine Biology. 1985;32:19-32.
952 89. Cole JJ. Plumbing the global carbon cycle: integrating inland waters into the terrestrial
953 carbon budget. . Ecosystems. 2007;10:171-84.
954 90. Wohl E. Rivers in the Landscape: Science and Management. Colorado State University:
955 Wiley Blackwell; 2014.
956 91. Arthington AH, Naiman RJ, McClain ME, Nilsson C. Preserving the biodiversity and
957 ecological services of rivers: New challenges and research opportunities. Freshwater Biology.
958 2010;55(1):1-16.
959 92. Hamlet AF, Lettenmaier DP. Effects of climate change on hydrology and water resources in
960 the Columbia River basin. Journal of the American Water Resources Association. 1999;35(6):1297-
961 665.
962 93. Burla M, Baptista AM, Zhang J, Frolov S. Seasonal and interannual variability of the
963 Columbia River plume: A perspective enabled by multiyear simulation databases. Journal of
964 Geophysical Research. 2010;115(C2):1-25.
965 94. Kukulka T, Jay DA. Impacts of Columbia River discharge on salmonid habitat: 1. A
966 nonstationary fluvial tide model. Journal of Geophysical Research. 2003;108(C9):1-20.
967 95. Burger G, Schulla J, Werner AT. Estimates of future flow, including extremes of the
968 Columbia River headwaters. Water Resources Research. 2011;47(10).
969 96. Mantua NJ, Francis RC, Hare SR, Zhang Y, Wallace JM. A Pacific interdecadal climate
970 oscillation with impacts on salmon production. Bull Am Meteorol Society. 1997;78(6):1069-79.
971 97. Meybeck M. Global analysis of river systems: from Earth system controls to Anthropocene
972 syndromes. Philosophical Transactions of the Royal Society of London Series B: Biological
973 Sciences,. 2003;358(1440):1935.
974 98. Gounand I, Little CJ, Harvey E, Altermatt F. Cross-ecosystem carbon flows connecting
975 ecosystems worldwide. Nature Communications. 2018;9.
976 99. Hall RO, Tank JL, Baker MA, Rosi-Marshall EJ, Hotchkiss ER. Metabolism, gas exchange,
977 and carbon spiraling in rivers. Ecosystems. 2016;19:73-86.
978 100. Rose V, Rollwagen-Bollens G, Bollens S, Zimmerman J. The effects of run-of-river dam spill
979 on Columbia River microplankton. River Research and Applications. 2019;35:1478-88.
980 101. Rose V, Rollwagen-Bollens G, Bollens S, Zimmerman J. Seasonal and interannual variation
981 in lower Columbia River phytoplankton (2005-2018): Environmental variability and a decline in large
982 bloom-forming diatoms. Aquatic Microbial Ecology. 2021;87:29-46.
983 102. Oliver RL, Merrick CJ. Partitioning of river metabolism identifies phytoplankton as a major
984 contributor in the regulated Murray River (Australia). Freshwater Biol. 2006;51:1131-48.
985 103. Minshall GW. Interbiome comparison of stream ecosystem dynamics. Ecol Monogr.
986 1983;53:1-25.
987 104. Rehmann CR, Soupir ML. Importance of interactions between the water column and the
988 sediment for microbial concentrations in streams. Water Research. 2009;43(18):4579-89.

105. Accola K, Cordell J, Oxborrow B, Toft JD, Suzumura A, Grote J. Subyearling Chinook salmon diets in Lower Columbia River estuarine habitats. PLoS One. 2025;20(6):e0325939.
106. Iriarte A, Daneri G, Garcia VMT, Purdie DA, Crawford DW. Plankton community respiration and its relationship to chlorophyll a concentration in marine coastal waters. Oceanologica Acta. 1991;14(4):379-88.
107. Lopez-Sandoval DC, Rodriguez-Ramos T, Cermeno P, C. S, Maranon E. Photosynthesis and respiration in marine phytoplankton: Relationship with cell size, taxonomic affiliation and growth phase. J Exp Mar Biol Ecol. 2014;457:151-9.
108. Vona V, Di Martino Rigano V, Lobosco O, Carfagna S, Esposito S, Rigano C. Temperature responses of growth, photosynthesis, respiration and NADH: nitrate reductase in cryophilic and mesophilic algae. New Phytologist. 2004;163:325-31.
109. LeB Williams PJ, Quay PD, Westberry TK, Behrenfeld MJ. The oligotrophic ocean is autotrophic. Annual Reviews in Marine Science. 2012;5:535-49.
110. Robinson C, Williams PJL. Respiration and its measurement in the surface waters. In: del Giorgio PA, Williams PJL, editors. Respiration in Aquatic Ecosystems. New York: Oxford University Press; 2005. p. 147-80.
111. Small LF, Prahl FG. A particle conveyor belt process in the Columbia River estuary: Evidence from chlorophyll *a* and particulate organic carbon. Estuaries and Coasts. 2004;27:999-1013.
112. Crump BC, Fine LM, Fortunato CS, Herfort L, Needoba JA, Murdock S, et al. Quantity and quality of particulate organic matter controls bacterial production in the Columbia River estuary. Limnol Oceangr. 2017;62(6):2713-31.
113. Simenstad CA, Small LF, McIntire CD. Consumption processes and food web structure in the Columbia River Estuary. Progress in Oceanography. 1990;25(1-4):271-97.
114. Lara-Lara JR, Frey BE, Small LF. Primary production in the Columbia River Estuary II. Grazing losses, transport, and a phytoplankton carbon budget. Pacific Science. 1990;44(1):38-50.
115. Dexter E, Katz SL, Bollens SM, Rollwagen-Bollens G, Hampton SE. Modeling the trophic impacts of invasive zooplankton in a highly invaded river. PLoS One. 2020;15(12):e0243002.
116. Kagami M. Parasitic chytrids: their effects on phytoplankton communities and food-web dynamics. Hydrobiologia. 2007;578:113-29.
117. Maier MA, Peterson TD. Prevalence of chytrid parasitism among diatom populations in the lower Columbia River (2009-2013). Freshwater Biol. 2017;62(2):414-28.
118. Prahl FG, Small LR, Sullivan BA, Cordell J, Simenstad CA, Crump BC, et al. Biogeochemical gradients in the lower Columbia River. Hydrobiologia. 1998;361:37-52.
119. Pathak D, Hutchins M, Brown LE, Loewenthal M, Scarlett P, Armstrong L, et al. High-resolution water-quality and ecosystem-metabolism modeling in lowland rivers. Limnol Oceangr. 2022;67:1313-27.
120. Kirk JTO. The vertical attenuation of irradiance as a function of the optical properties of the water. Limnology and Oceanography. 2003;48(1):9-17.
121. Babin M, Therriault JC, Legendre L, Condal A. Variations in the Specific Absorption Coefficient for Natural Phytoplankton Assemblages: Impact on Estimates of Primary Production. Limnology & Oceanography. 1993;38(1):154-77.
122. Tranvik LJ. Allochthonous dissolved organic matter as an energy source for pelagic bacteria and the concept of the microbial loop. Hydrobiologia. 1992;229:107-14.
123. Bristow MPF, Bundy DH, Edmonds CM, Ponto PE, Frey BE, Small LF. Airborne laser fluorosensor survey of the Columbia and Snake rivers: simultaneous measurements of chlorophyll, dissolved organics and optical attenuation. International Journal of Remote Sensing. 1985;6:1707-34.
124. Bernhardt ES, Savoy P, Vlah MJ, Appling AP, Koenig LE, Hall Jr. RO, et al. Light and flow regimes regulate the metabolism of rivers. Proc Natl Acad Sci USA. 2022;119:e2121976119.

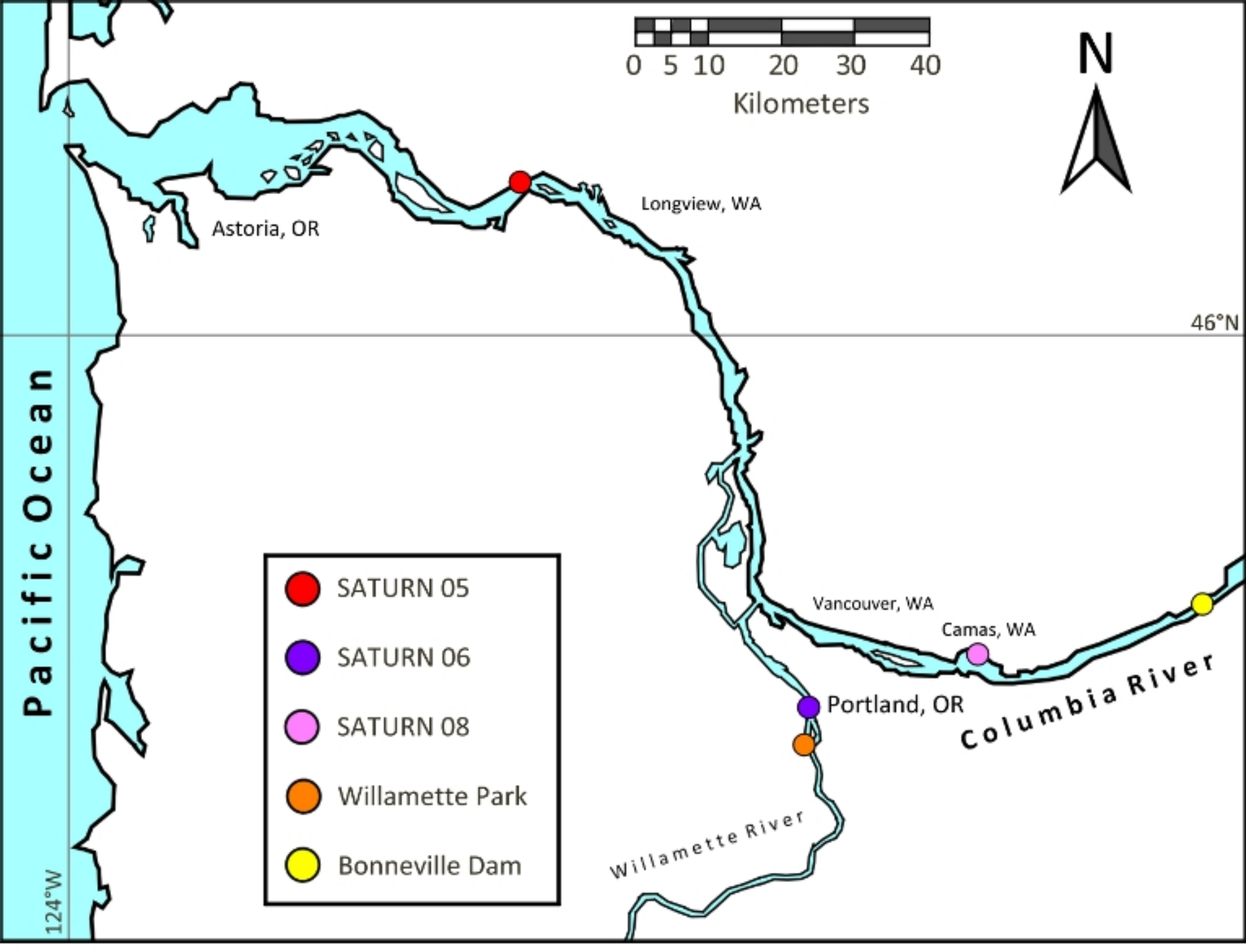
0 5 10 20 30 40
Kilometers
N
Longview, WA
Astoria, OR
46°N
Pacific Ocean
SATURN 05
SATURN 06
SATURN 08
Willamette Park
Bonneville Dam
Vancouver, WA
Camas, WA
Portland, OR
Columbia River
Willamette River
124°W

Figure 1

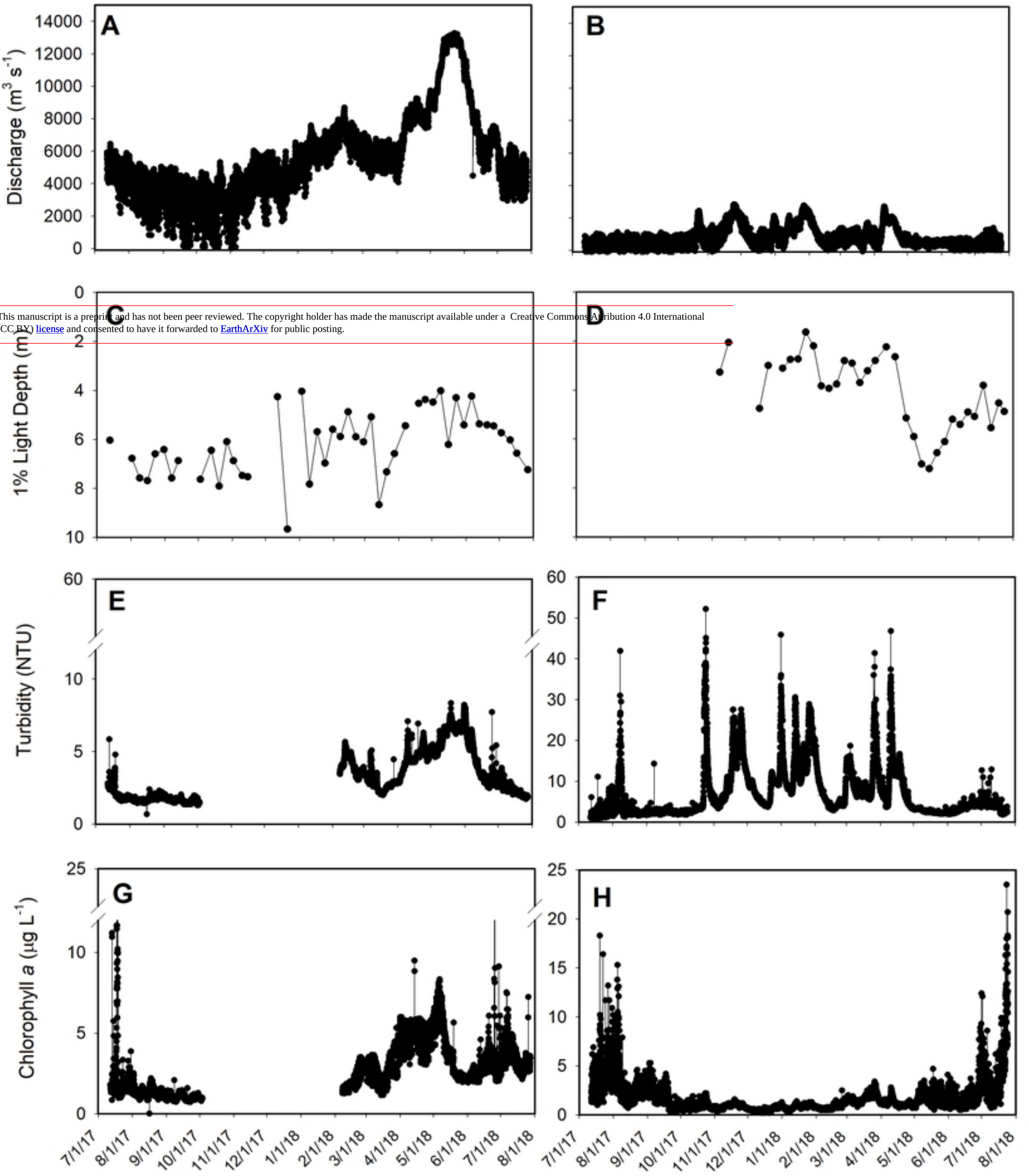

Figure 2

Figure 5

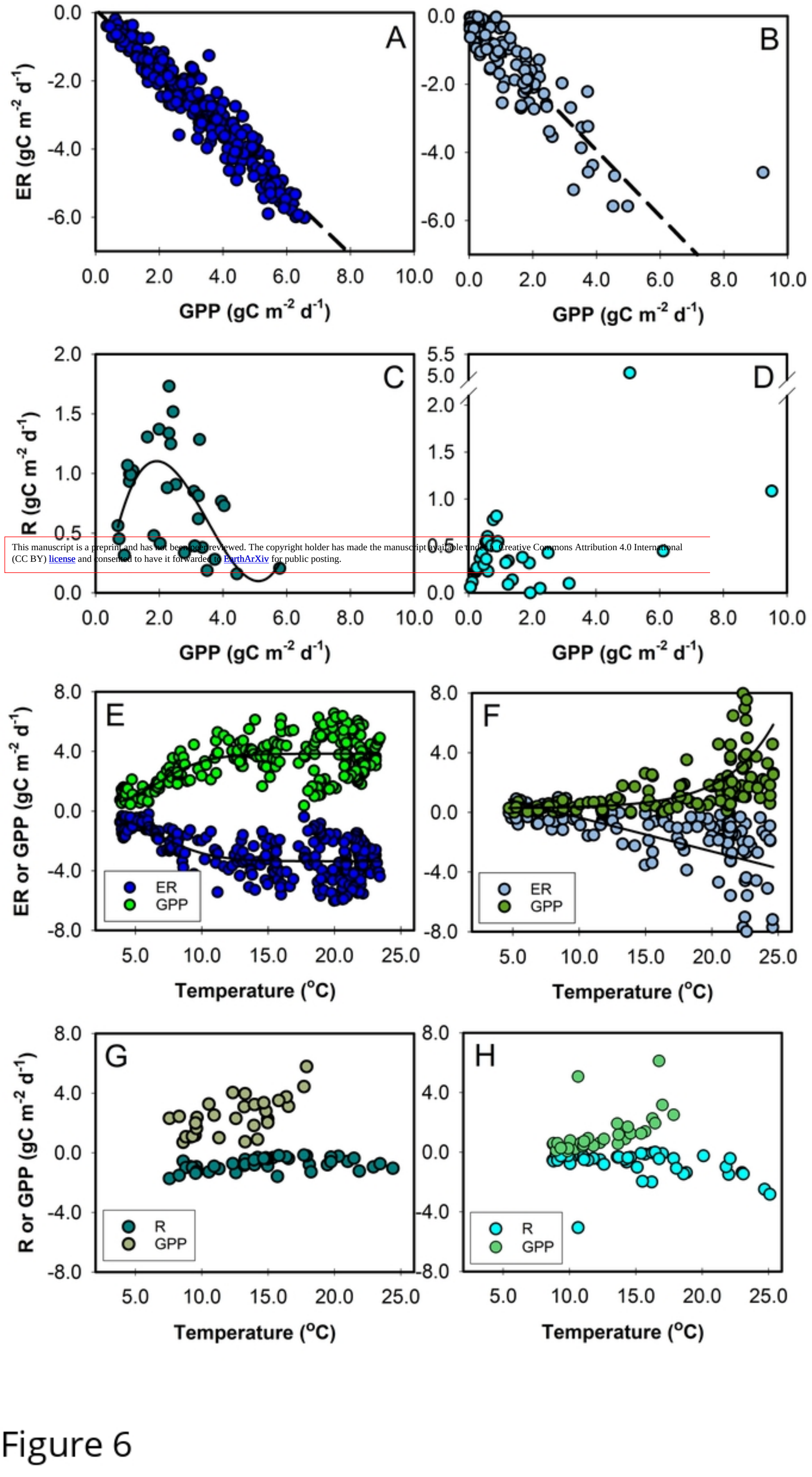

Figure 6

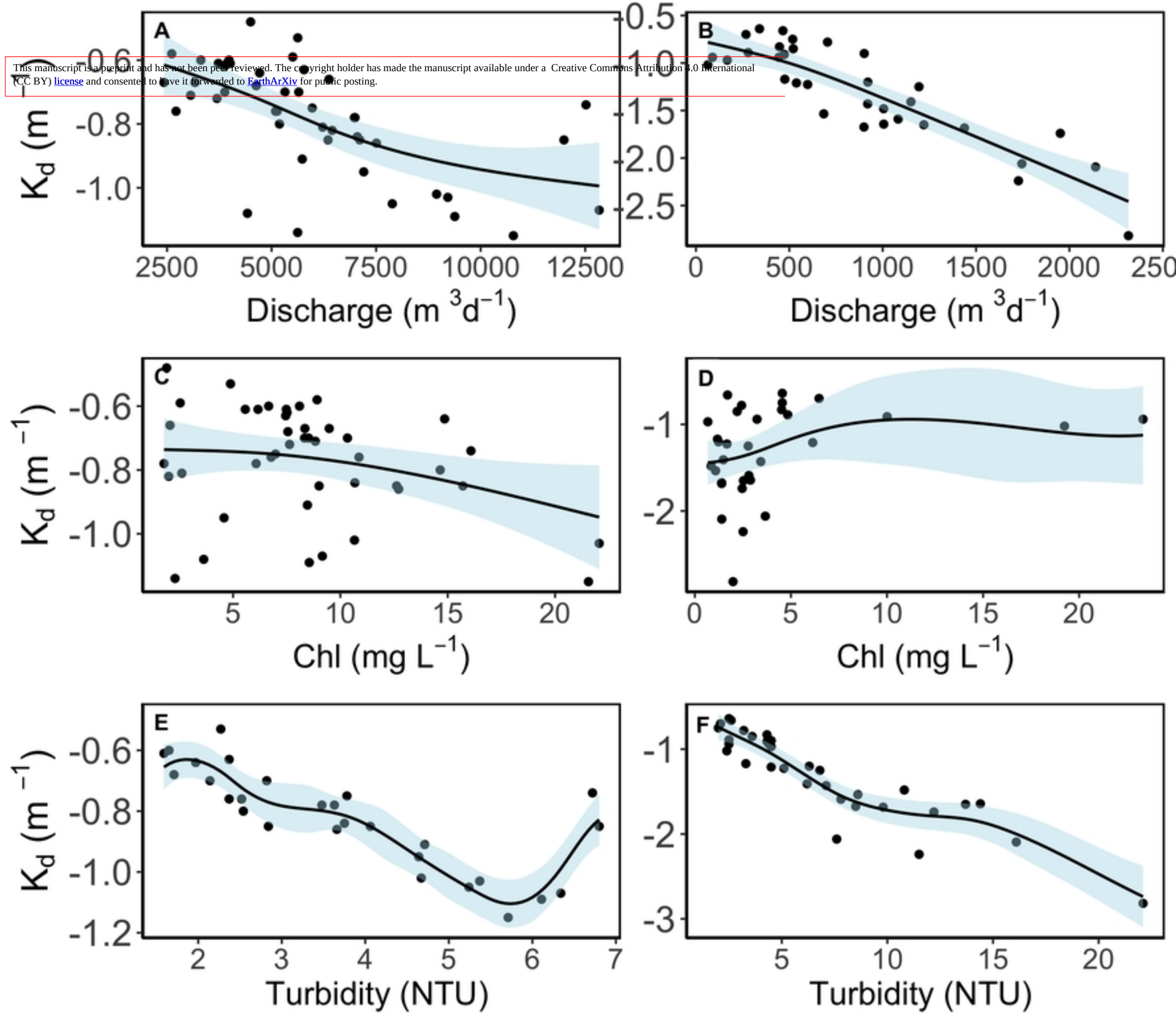

Figure 3

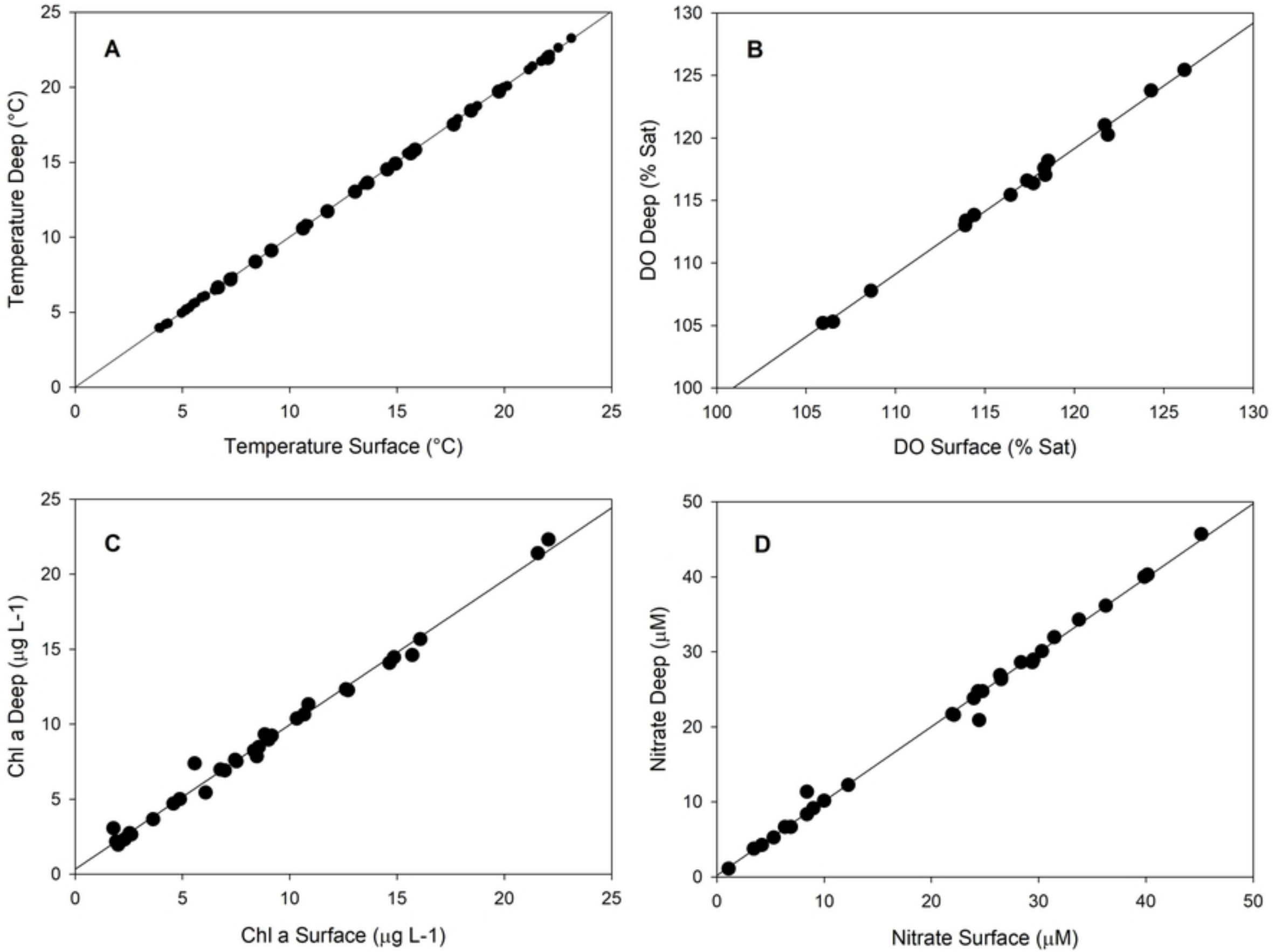

Figure 4

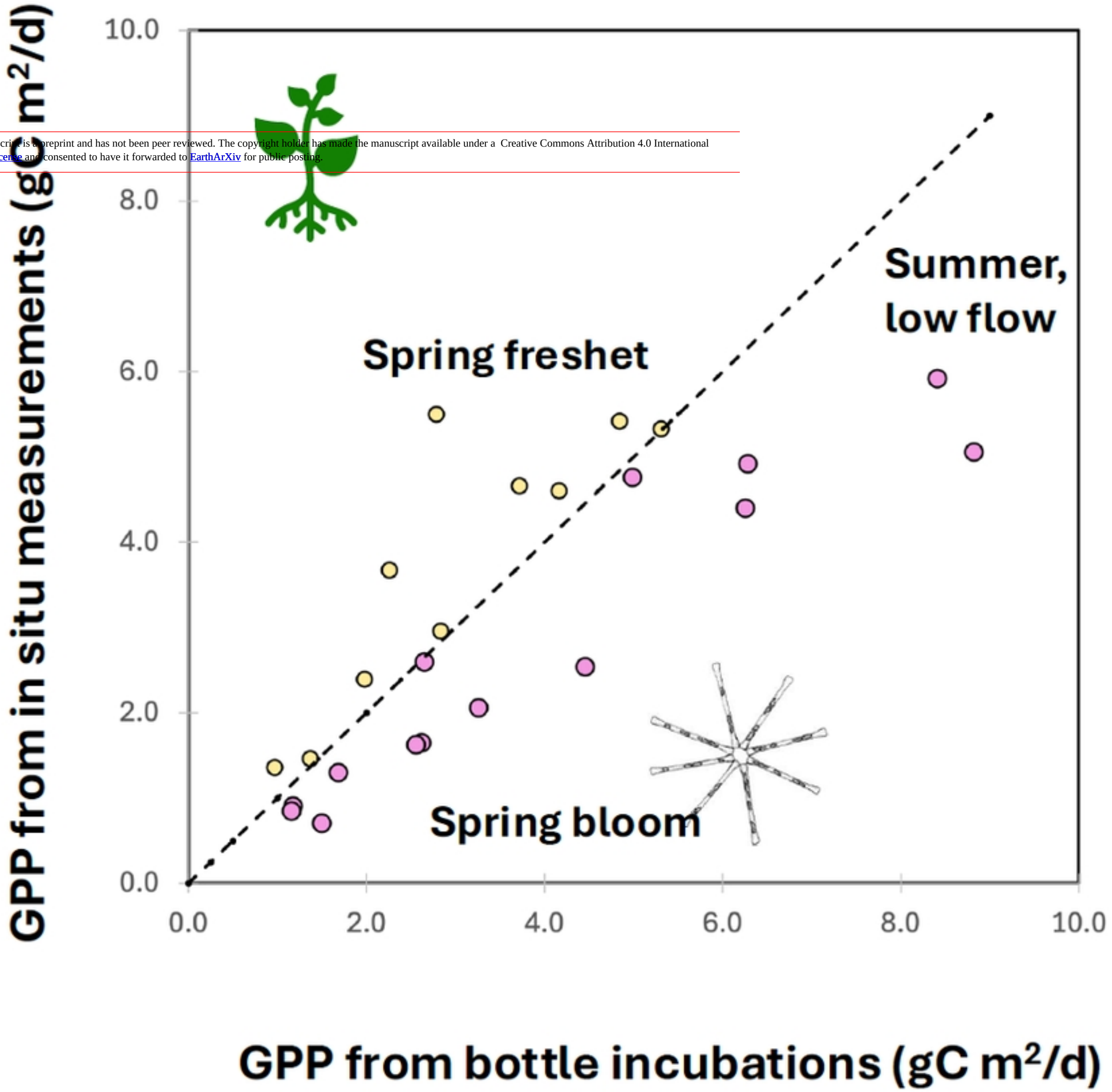

Figure 9

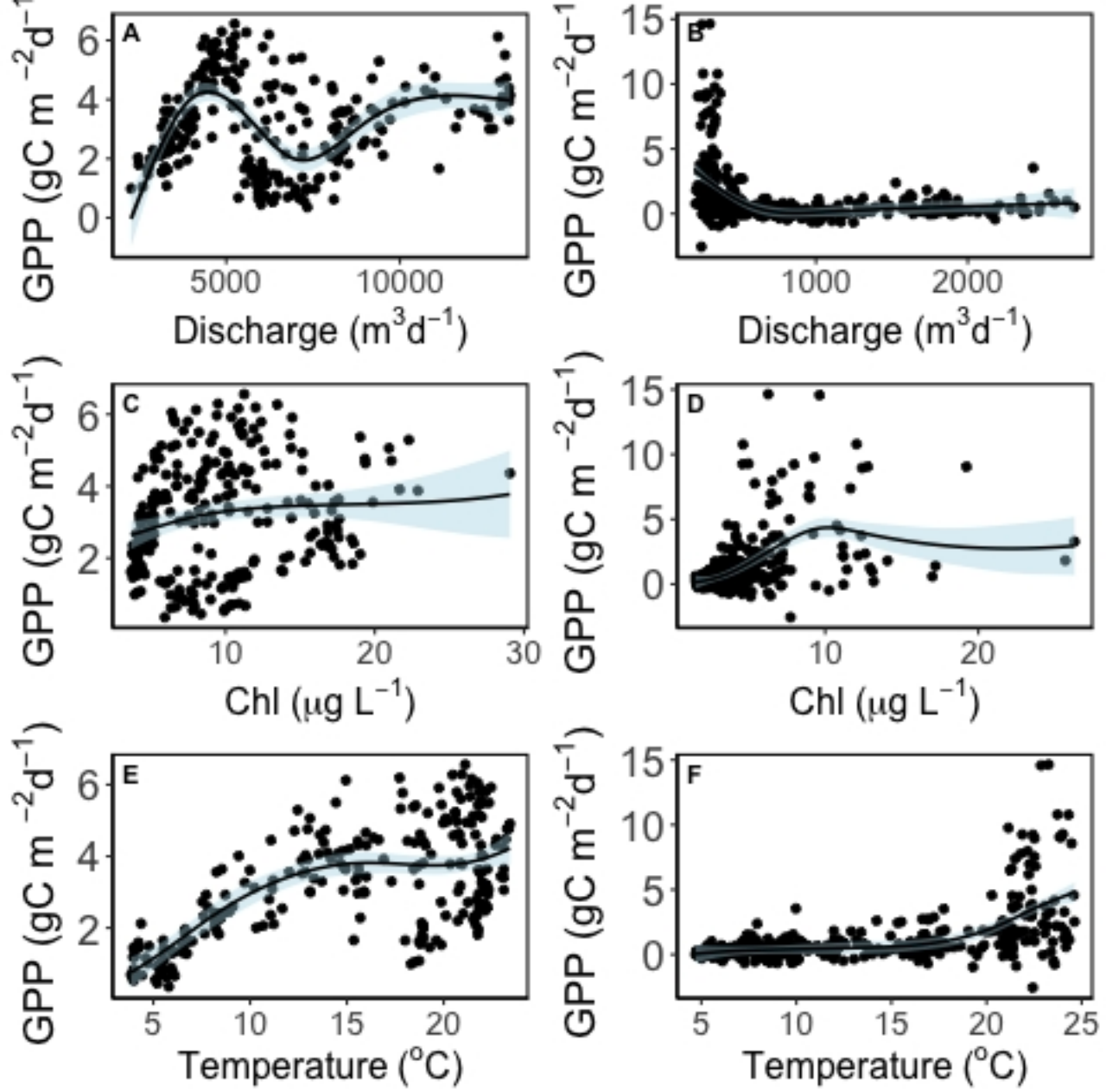
A
B
C
D
E
F
GPP (gC m^{-2}d^{-1})
Discharge (m^{3}d^{-1})
Chl (μg L^{-1})
Temperature (°C)
0
2
4
6
5000
10000
1000
2000
10
20
30
5
15
25

Figure 7

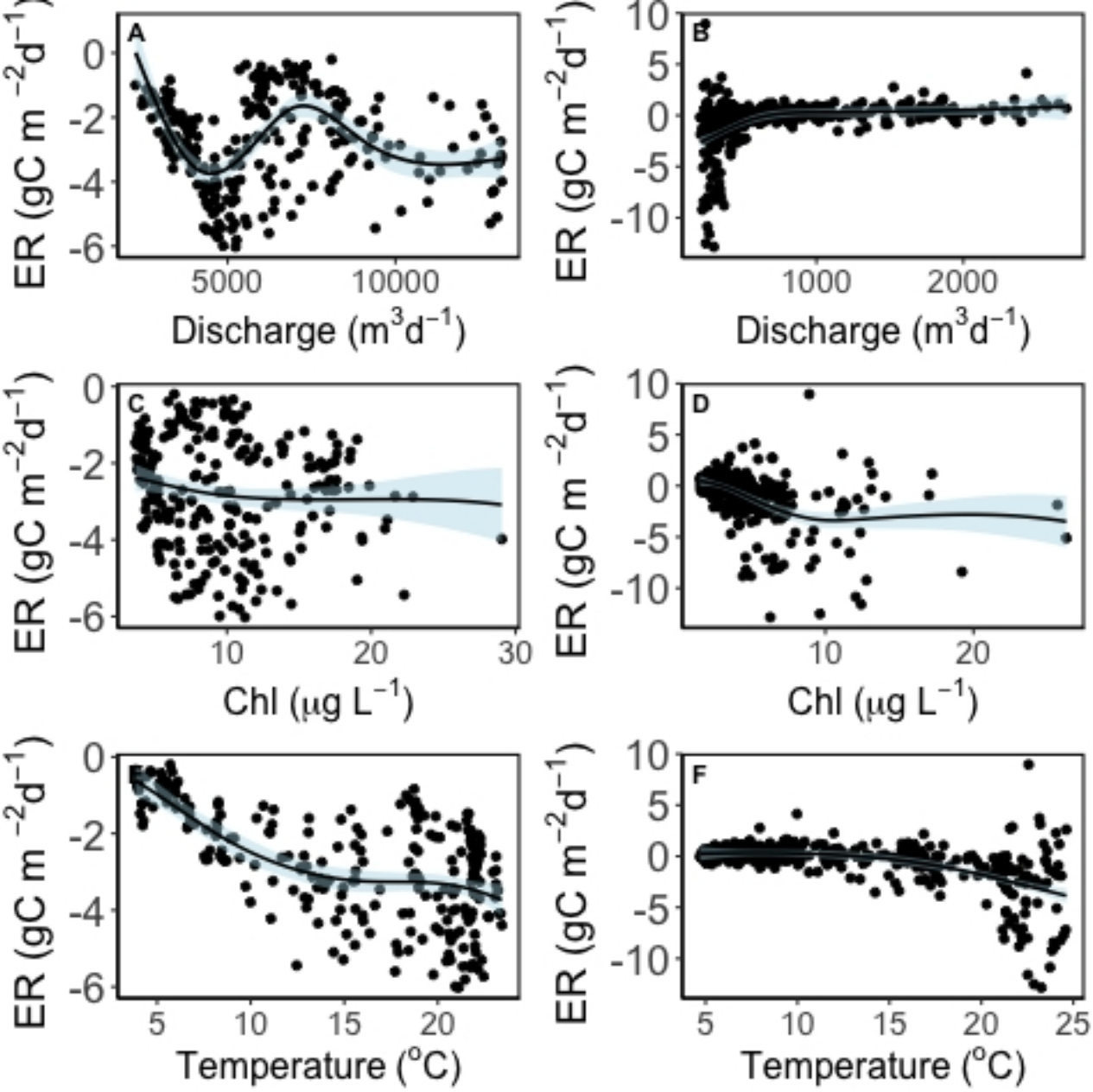
A
B
C
D
F
ER (gC m^{-2}d^{-1})
Discharge (m^{3}d^{-1})
Chl (μg L^{-1})
Temperature (°C)
0
-2
-4
-6
10
5
0
-5
-10
5000
10000
1000
2000
10
20
30
5
10
15
20
25

Figure 8